because it integrates into the host genome in a variety of dividing and non-dividing cells. Because the dystrophin complementary DNA is too large to be incorporated into a lentiviral vector, a truncated but fully functional version of the dystrophin complementary DNA[24–27] has to be used instead of the full-length one. When compared with conventional transfection of myogenic cells with large dystrophin-coding plasmids[28] or nucleofection in combination with ϕC31 integrase,[29] transfection by lentiviral vectors led to much more efficient expression of mini- or micro-dystrophin in *mdx* mice,[30] in non-human primate cells, and in human myogenic cells.[31] Lentiviral vectors were also used for introducing the therapeutic genes into other types of stem cells. Bachrach *et al.* reported expression of human micro-dystrophin in *mdx*^{5cv} muscles after systemic delivery of autologous side population cells modified with lentiviral vectors expressing micro-dystrophin.[32] Sampaolesi *et al.* reported intra-arterial delivery of autologous mesoangioblasts corrected by lentiviral vectors expressing α-sarcoglycan (α-SG), resulting in many α-SG-positive fibers, and morphological and functional recovery in downstream muscles of α-SG-null dystrophic mice.[33] A more recent study reported the autologous transplantation into skeletal muscle, of monkey muscle precursor cells transduced with micro-dystrophin by lentiviral vectors.[31] However, whether *ex vivo* gene therapy using lentiviral vectors expressing micro-dystrophin is indeed beneficial in large animal models such as dystrophic dogs, is still subject to controversy.[34]

Previously, Fukada *et al.* established a method of direct purification of quiescent satellite cells from adult mouse skeletal muscles, using fluorescence activated cell sorting (FACS) and a novel monoclonal antibody named SM/C-2.6.[35] The method is simple, and is expected to be applicable to the isolation of satellite cells from dystrophic (autologous) muscles for cell therapy.

In this study, we first directly isolated satellite cells from *mdx* mice using the SM/C-2.6 antibody and FACS. We showed that *mdx*-SM/C-2.6$^+$ cells transduced with lentiviral vectors expressing micro-dystrophin efficiently contributed to regeneration of *mdx* muscles and expressed micro-dystrophin at the sarcolemma when grafted. Our results indicate that the autologous satellite cell isolated by the SM/C-2.6 antibody and genetically corrected by a lentiviral vector is a feasible tool for cell therapy of DMD or of localized forms of muscular dystrophy.

RESULTS

Passaged SM/C-2.6$^+$ satellite cells show reduced regenerative capacity

We isolated satellite cells from the limb muscles of 8–12-week-old C57BL/6 mice using FACS and a novel monoclonal antibody, SM/C-2.6.[35] A previous study has shown that satellite cells are highly enriched in the SM/C-2.6$^+$ fraction.[35] Immediately after isolation by FACS, SM/C-2.6$^+$ cells expressed Pax7, but not MyoD, myogenin, or Ki67 (**Table 1**). After 4 days of culture, more than 95% of the cells expressed MyoD and Ki67 (data not shown). Pax7 marks quiescent, activated satellite cells and their progeny, myoblasts,[36] whereas MyoD marks activated satellite cells and myoblasts.[37,38] Ki67 is a marker of proliferating cells. It follows, therefore, that SM/C-2.6$^+$ cells are highly purified satellite cells in the G_0 phase immediately after isolation from muscle tissues.

Table 1 Expression of myogenic and proliferative markers of freshly isolated SM/C-2.6$^+$ cells from limb muscles of C57BL/6 or *mdx* mice

Marker	B6-SM/C-2.6$^+$ cells (%)	*mdx*-SM/C-2.6$^+$ cells (%)
Pax7	95 ± 1.4	94 ± 2.1
MyoD	0 ± 0	19 ± 2.8
Myogenin	0 ± 0	7 ± 1.3
Ki67	0.6 ± 1.0	34 ± 1.8

The expression level of each marker is shown as the percentage of positive cells in total cells stained with 4′,6-diamidino-2-phenylindole in three randomly selected fields. Data are represented as mean values ± SD.

To investigate the regenerative efficiency of SM/C-2.6$^+$ satellite cells when grafted into mouse skeletal muscles, three kinds of cells were prepared from limb muscles of 8–12-week-old GFP-Tg mice: (i) quiescent SM/C-2.6$^+$ cells freshly isolated by FACS (**Figure 1a**), (ii) expanded SM/C-2.6$^+$ cells *in vitro* with or without passaging (**Figure 1a**), and (iii) cultured primary myoblasts isolated by a conventional pre-plating method.[39] These cells were injected at 2×10^4 cells per muscle into the tibialis anterior (TA) muscle of 8–12-week-old C57BL/6 and 5-week-old dystrophin-deficient *mdx* mice. Twenty four hours before cell transplantation the recipient C57BL/6 muscles were injected with cardiotoxin (CTX) so as to induce regeneration. Four weeks after the injection, we investigated the contribution of each cell population to muscle regeneration by immunodetection of GFP-positive fibers. Freshly isolated SM/C-2.6$^+$ cells (**Figure 1b**) produced many more GFP-positive fibers than those produced by the same number of cultured SM/C-2.6$^+$ cells passaged once *in vitro* (**Figure 1c**, passage 1). We next examined the effects of expansion, without passaging and with repeated passaging, on the regenerative capacity of the cells. The number of GFP-positive myofibers derived from GFP-Tg SM/C-2.6$^+$ cells dropped considerably after first passage *in vitro* and then gradually decreased with subsequent passages in both CTX-injected C57BL/6 mice (**Figure 1d**) and in *mdx* mice (**Figure 1e**). Primary myoblasts prepared by the pre-plating method[39] also showed low regenerative capacity (**Figure 1d**). Surprisingly, the regenerative efficiency of cells expanded *in vitro* without passaging was comparable to that of freshly isolated cells (**Figure 1d** and **e**). These results suggested to us that it is possible to genetically correct dystrophin-deficient satellite cells *ex vivo* before transplantation without causing a reduction in their regenerative capacity.

In order to know why fresh or "expansion" cells gave rise to more myofibers when compared with cells passaged *in vitro*, we compared the colony formation ability of fresh satellite cells with that of passaged myoblasts (passage 1). The results showed that fresh satellite cells formed larger colonies than passage 1 cells, when plated at a density of 1 cell/well on 96-well plates, although the rate of colony formation was not significantly different between these two cells (fresh, 26% versus passage 1, 23%) (**Supplementary Figure S1**). In contrast, there was no difference in fusion index between fresh satellite cells and passaged myoblasts (data not shown). Collectively, a reduction in the proliferative ability of passaged myoblasts *in vitro* might partly explain their lower regenerative capacity *in vivo*.

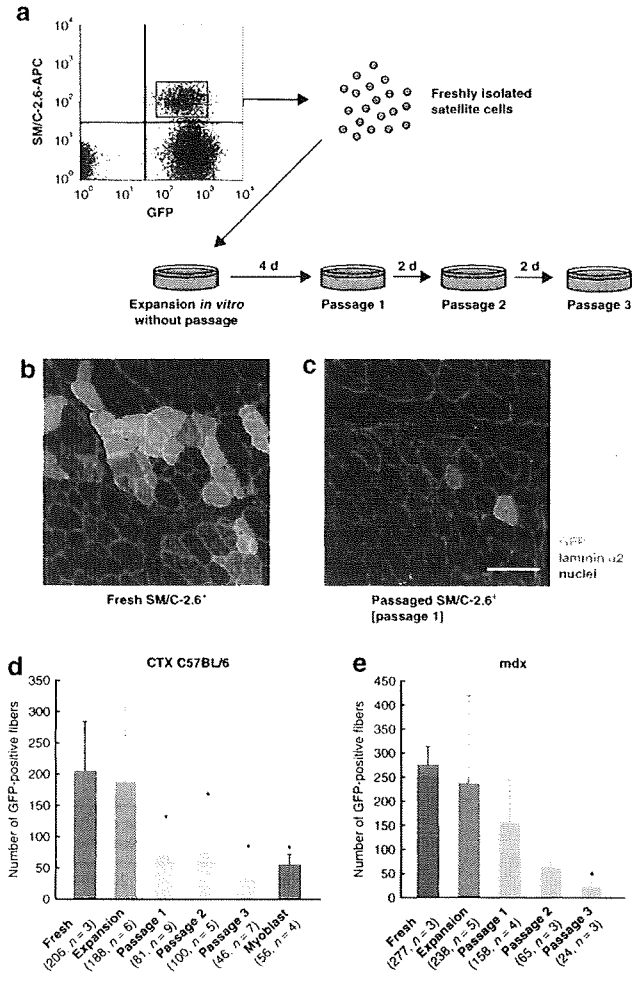

Figure 1 The regenerative capacity of SM/C-2.6$^+$ satellite cells isolated from adult mouse skeletal muscles by fluorescence activated cell sorting (FACS). (**a**) Flow cytometry of mononucleated cells derived from limb muscles of green fluorescent protein-transgenic (GFP-Tg) mice after staining with SM/C-2.6 antibody and culture conditions of sorted cells. SM/C-2.6$^+$ GFP$^+$ cells (red square) were sorted as the satellite cell fraction. These cells were cultured in proliferation medium for 4 days (expansion *in vitro* without passage) and then passaged up to three times at 2-day intervals. (**b**) Freshly isolated and (**c**) passaged SM/C-2.6$^+$ cells (passage 1) from GFP-Tg mice were injected into C57BL/6 tibialis anterior (TA) muscles. The muscles were treated with cardiotoxin (CTX) 24 hours before cell transplantation and then injected with 2×10^4 cells per TA muscle. Four weeks after the injection, cross-sections were stained with anti-GFP (green) and laminin α2 (red) antibodies. Nuclei were stained with TOTO3 (blue). Bar: 80 μm. (**d**, **e**) Comparison of muscle regenerative efficiencies of three kinds of cells prepared from GFP-Tg mice: (i) quiescent SM/C-2.6$^+$ cells freshly isolated by FACS (red bars), (ii) expanded SM/C-2.6$^+$ cells *in vitro* without passaging (orange bars) or passaged SM/C-2.6$^+$ cells (yellow bars with passage numbers), and (iii) primary myoblasts isolated by the preplating method (blue bar in **d**). The same numbers of cells (2×10^4 cells) were grafted into TA muscles of CTX-treated C57BL/6 (d) and *mdx* mice (**e**). The number of GFP-positive fibers per cross-section was counted after staining with anti-GFP antibody. Error bars represent SD. $^*P < 0.05$ compared with freshly isolated SM/C-2.6$^+$ cells.

SM/C-2.6$^+$ satellite cells transduced with lentiviral vectors efficiently contribute to muscle regeneration

Successful gene and cell therapy for DMD requires sustained expression of the therapeutic gene in striated muscle. The

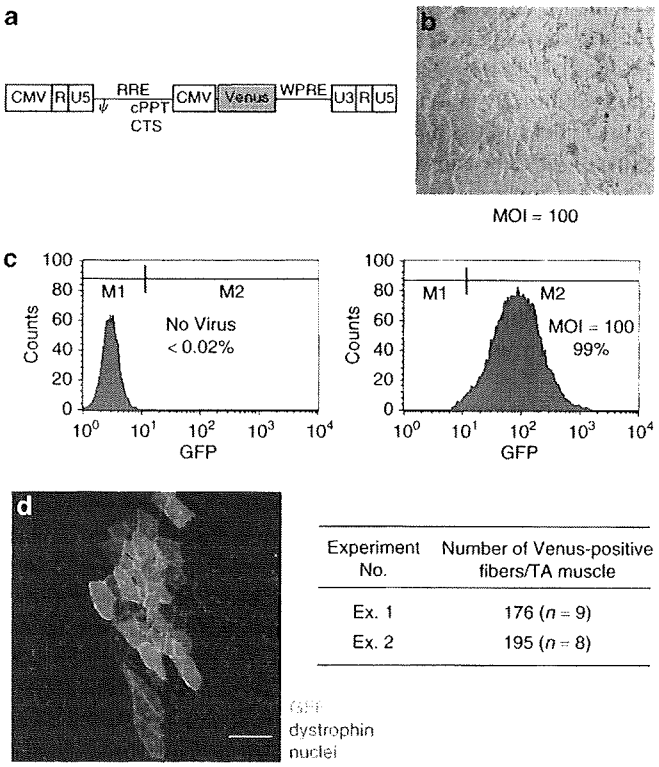

Experiment No.	Number of Venus-positive fibers/TA muscle
Ex. 1	176 (n = 9)
Ex. 2	195 (n = 8)

Figure 2 Lentiviral vector-mediated gene transfer into SM/C-2.6$^+$ satellite cells and transplantation of transduced cells into *mdx* mouse muscles. (**a**) Structure of the lentiviral vector expressing Venus under the control of a cytomegalovirus (CMV) promoter. (**b**) Fluorescence of Venus-expressing satellite cell-derived myoblasts. Freshly isolated SM/C-2.6$^+$ cells from C57BL/10 limb muscles were transduced with lentiviral vectors expressing Venus at a multiplicity of infection (MOI) of 100 for 16 hours, and cultured in proliferation medium for 3 days. (**c**) Flow cytometric analysis of non-transduced (left panel) and transduced (right panel) SM/C-2.6$^+$ cells 3 days after the transduction. M2 denotes the area of Venus-expressing cells. At a MOI of 100, 99% of the cells expressed Venus. (**d**) Venus- and dystrophin-positive fibers formed by SM/C-2.6$^+$ cells transduced with lentiviral vectors *in vitro*. Transduced cells (2×10^4) were injected into tibialis anterior (TA) muscles of *mdx* mice. Four weeks after the injection, cross-sections were stained with anti-GFP (green) and dystrophin (red) antibodies. Nuclei were stained with TOTO3 (blue). The number of Venus-positive fibers per cross-section was counted. Bar: 80 μm. cPPT, central polypurine tract; CTS, central termination sequence; GFP, green fluorescent protein; RRE, rev responsive element; WPRE, woodchuck hepatitis virus post-transcriptional regulatory element.

lentiviral vector can carry a relatively large transgene and integrate it into the genome of non-dividing cells such as quiescent satellite cells. We therefore attempted lentiviral vector–mediated gene transfer into satellite cells. For this purpose, we used a human immunodeficiency virus-1–based lentiviral vector pseudotyped with vesicular stomatitis virus-G glycoprotein.[40] To start with, we used a vector that expresses Venus, a variant of yellow fluorescent protein[41] under the control of a cytomegalovirus (CMV) promoter (**Figure 2a**). Freshly isolated satellite cells from limb muscles of 8–12-week-old C57BL/10 mice, which are syngenic to *mdx*, were transduced with the lentiviral vectors at a multiplicity of infection (MOI) of 100 for 16 hours. After removal of free viral vectors and *in vitro* expansion of the cells for 3 days, numerous Venus-positive cells were detected (**Figure 2b**). Flow

cytometric analyses revealed that 99% of the SM/C-2.6$^+$ satellite cell–derived myoblasts expressed Venus when transduced at a MOI of 100 (**Figure 2c**, right panel). These transduced cells were injected into TA muscles of 5-week-old *mdx* mice at 2×10^4 per muscle. Four weeks after the injection, the muscle regeneration capacity of cells transduced with lentiviral vectors was investigated by immunodetection of Venus- or dystrophin-positive fibers. As in the case of the non-transduced cells (**Figure 1d** and **e**), grafting of transduced cells too led to many Venus- and dystrophin-positive fibers (**Figure 2d**). This serves to show that SM/C-2.6$^+$ satellite cell-derived myoblasts transduced with lentiviral vectors contribute efficiently to muscle regeneration.

Direct isolation of SM/C-2.6$^+$ satellite cells from dystrophic muscles of *mdx* mice

In order to test whether autologous myogenic precursor cells genetically corrected to express a dystrophin gene represent a possible tool in DMD therapy, we next attempted to directly isolate SM/C-2.6$^+$ cells from limb muscles of 5-week-old *mdx* mice. Numerous inflammatory and fibroblastic cells reflecting the active cycles of the degeneration–regeneration process are found in dystrophic muscles. SM/C-2.6 antibody reacts with activated fibroblastic cells (Fukada *et al.*, unpublished data). Because satellite cells are negative for both Sca-1 and CD31,[35] we stained *mdx* muscle-derived mononuclear cells with a cocktail of CD45, CD31, Sca-1, and SM/C-2.6 antibodies and collected SM/C-2.6$^+$ CD45$^-$ CD31$^-$ Sca-1$^-$ cells as the satellite cell fraction (**Figure 3a**). When these cells were cultured in proliferation medium for 4 days, more than 95% of them expressed MyoD (**Figure 3b**). These results indicate that, using the SM/C-2.6 antibody, a pure population of satellite cells can be isolated, not only from wild-type muscle but also from dystrophic muscle of *mdx* mice. Immediately after isolation, the majority of satellite cells from C57BL/6 mice were negative for MyoD, myogenin, and Ki67. On the other hand, 19% of *mdx*-satellite cells were positive for MyoD and 34% of the cells were positive for Ki67 (**Table 1**). There was no difference between *mdx*- and B6-SM/C-2.6$^+$ cells with respect to expression of Pax7 (**Table 1**). This proves that a considerable fraction of satellite cells are in an activated, proliferative state in skeletal muscles of *mdx* mice.

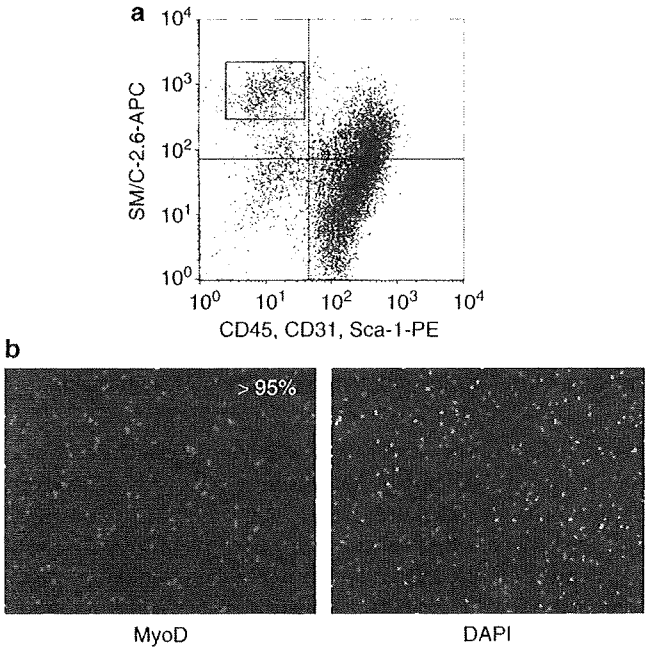

Figure 3 Direct isolation of SM/C-2.6$^+$ satellite cells from dystrophic muscles of *mdx* mice. (**a**) Flow cytometry of mononucleated cells derived from *mdx* mice, and stained with a cocktail of CD45, CD31, Sca-1, and SM/C-2.6 antibodies. SM/C-2.6$^+$ CD45$^-$ CD31$^-$ Sca-1$^-$ cells (red square) were sorted as the satellite cell fraction. (**b**) Sorted *mdx*-satellite cells were cultured in proliferation medium for 4 days and stained with anti-MyoD antibody (green) and 4′,6-diamidino-2-phenylindole (DAPI) (nuclei, blue). More than 95% of them expressed MyoD.

Successful micro-dystrophin gene transfer into *mdx*-SM/C-2.6$^+$ satellite cells

The full-length dystrophin complementary DNA, at 14 kilobase (kb), is too large to be incorporated into a lentiviral vector. In previous studies, we constructed a rod-truncated micro-dystrophin *CS1* and demonstrated that it effectively rescued

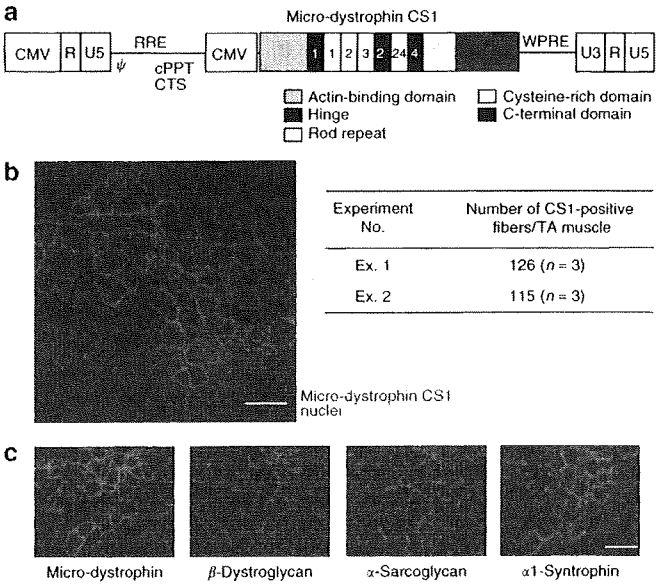

Figure 4 Lentiviral vector-mediated micro-dystrophin *CS1* gene transfer into *mdx*-SM/C-2.6$^+$ cells and transplantation of transduced cells into *mdx* muscles. (**a**) Structure of the lentiviral vector expressing micro-dystrophin *CS1*. *CS1* complementary DNA was inserted downstream of the cytomegalovirus (CMV) promoter. *CS1* has the N-terminal domain, a shortened version of the central rod domain with four rod repeats and three hinges, the cysteine-rich domain, and the C-terminal domain. The numbers of rod repeats and hinges are also shown. (**b**) Freshly isolated SM/C-2.6$^+$ cells from *mdx* dystrophic muscles were transduced with lentiviral vectors expressing micro-dystrophin *CS1* at a multiplicity of infection of 200 for 16 hours and cultured in proliferation medium for 2 days. Transduced cells (2×10^4) were injected into *mdx* tibialis anterior (TA) muscles. Four weeks after the injection, cross-sections were stained with anti-dystrophin antibody (red) and TOTO3 (nuclei, blue). The number of micro-dystrophin *CS1*-positive fibers per cross-section was counted. Bar: 80 μm. (**c**) Restoration of dystrophin-associated proteins at the sarcolemma of micro-dystrophin-positive fibers. Serial cross-sections were stained with anti-dystrophin, β-dystroglycan, α-sarcoglycan, and α1-syntrophin antibodies (red), and TOTO3 (nuclei, blue). Bar: 80 μm. cPPT, central polypurine tract; CTS, central termination sequence; RRE, rev responsive element; WPRE, woodchuck hepatitis virus post-transcriptional regulatory element.

the dystrophic phenotypes of *mdx* mice when introduced as a transgene[24] or by adeno-associated viral vectors.[25] We therefore inserted a 4.9 kb micro-dystrophin *CS1* into the lentiviral vector as a therapeutic gene. Freshly isolated *mdx*-SM/C-2.6$^+$ cells were transduced with lentiviral vectors expressing micro-dystrophin *CS1* under the control of a CMV promoter (**Figure 4a**) at a MOI of 200 for 16 hours. In this condition, 97% of the cells expressed micro-dystrophin *CS1* (data not shown). These transduced cells were injected into TA muscles of 5-week-old *mdx* mice at 2×10^4 cells per muscle. Four weeks after the injection, the muscle regeneration capacity of the cells was investigated by immunodetection of micro-dystrophin-positive fibers. Many myofibers expressed micro-dystrophin *CS1* on the sarcolemma at an average of 120 fibers per muscle (**Figure 4b**). Further, we examined the restoration of the dystrophin-associated protein complex in micro-dystrophin-positive fibers by immunodetection of α-SG, β-dystroglycan, and α1-syntrophin. As shown in **Figure 4c**, all these proteins were expressed at the sarcolemma of micro-dystrophin *CS1*-positive myofibers, thereby suggesting the recovery of dystrophin-associated protein complex by the introduction of micro-dystrophin. These results indicate that *mdx*-SM/C-2.6$^+$ cells transduced with lentiviral vectors expressing micro-dystrophin *CS1* efficiently contribute to regeneration of dystrophic muscles of *mdx* mice and restore the expression of the dystrophin/dystrophin-associated protein complex. It therefore follows that transplantation of autologous myogenic precursor cells prepared using the SM/C-2.6 antibody and genetically corrected by a lentiviral vector, is a possible approach for cell therapy in DMD or in localized forms of muscular dystrophy.

DISCUSSION

In vitro *passaging reduced the regenerative capacity of satellite cells*: In the present study, we directly isolated satellite cells from skeletal muscles of wild-type and *mdx* mice using SM/C-2.6, a novel monoclonal antibody,[35] and flow cytometry. Almost all satellite cells prepared from normal muscle are negative for MyoD, myogenin, and Ki67 immediately after isolation, thereby indicating that they are in a quiescent state. In contrast, approximately 20% of *mdx*-satellite cells are positive for MyoD and 35% are positive for Ki67 (**Table 1**). This result indicates that a fraction of *mdx*-satellite cells are already in an activated state.

Transplantation experiments showed that freshly isolated SM/C-2.6$^+$ satellite cells possess a higher capacity for muscle reconstitution when compared with SM/C-2.6$^+$ myoblasts passaged *in vitro* prior to transplantation. This result indicates that passaging and subsequent proliferation of satellite cells in culture reduce their intrinsic capacity for muscle reconstitution. In order to clarify the mechanisms of low myogenicity of passaged cells, we performed a colony-forming assay of freshly isolated satellite cells and passaged satellite cell-derived myoblasts (passage 1). When the cells were seeded at a density of 1 cell/well on 96-well plates, fresh satellite cells formed larger colonies than "passage 1" myoblasts (**Supplementary Figure S1**). In contrast, there was no difference in fusion index between these two cell populations (data not shown). Collectively, reduced efficiency of muscle fiber regeneration by passaged myoblasts can be partly explained by gradual loss of proliferative ability during passaging.

Importantly, we also found that satellite cells that were expanded *in vitro* without passaging showed regenerative capacity comparable to freshly isolated satellite cells. We therefore hypothesized that it might be possible to introduce therapeutic genes into satellite cells *in vitro* by a lentiviral vector before transplantation without causing any reduction in their regenerative capacity.

Comparison of regenerative capacity of SM/C-2.6$^+$ satellite cells with other reports: Previously, Montarras *et al.* directly isolated (Pax3) GFP-expressing satellite cells, which constitute a homogeneous population of small, non-granular, CD34$^+$ CD45$^-$ Sca-1$^-$ cells, from diaphragms of adult *Pax3*$^{GFP/+}$ mice by flow cytometry, and examined their regenerative capacity.[23] The researchers concluded that *in vitro* expansion of freshly isolated satellite cells for a few days prior to transplantation is a disadvantageous approach, because such satellite cell-derived myoblasts displayed considerably lower muscle regenerative efficiency than fresh satellite cells. In contrast, we observed no reduction in regenerative capacity as a result of *in vitro* expansion of freshly isolated satellite cells without passaging, although their capacity was remarkably reduced after passaging (**Figure 1d** and **e**). The discrepancy between the results of Montarras *et al.* and our results may be due to differences in the culture conditions employed. One possible explanation could be that our culture medium contained basic fibroblast growth factor. It has been reported that addition of basic fibroblast growth factor to culture medium improves transplantation efficiency.[42,43] The modification of culture conditions may enable maintenance of the intrinsic muscle regenerative capacity of satellite cells.

Previous muscle transplantation experiments utilized the progeny of satellite cells enzymatically dissociated from myofibers and extensively cultured to increase their numbers.[15,20–22] When 5×10^5 to 1×10^6 myoblasts taken from normal mice and prepared by the pre-plating method were transplanted into non-irradiated muscles of *mdx* mice, it resulted in fewer than 100 dystrophin-positive myofibers per muscle.[21] On the other hand, when 5×10^5 cells were injected into muscles of immunodeficient *mdx nu/nu* mice that had been pre-irradiated to ablate endogenous satellite cell function, they formed an average of 328 dystrophin-positive fibers.[18] Furthermore, grafting of 2×10^4 satellite cells freshly isolated from *Pax3*$^{GFP/+}$ mice into pre-irradiated TA muscles of *mdx nu/nu* mice led to dystrophin expression in an average of 587 fibers.[23] In our experiment, the same number (2×10^4) of satellite cells freshly isolated from adult normal mice gave rise to an average of only 277 myofibers in non-irradiated *mdx* muscles (**Figure 1d** and **e**). This shows that grafted muscle precursor cells form a far greater number of dystrophin-positive fibers in irradiated muscle than in non-irradiated muscle. The use of immunosuppressants such as FK506 also greatly improves the efficiency of transplantation.[7] In the present study, we injected myogenic cells into non-irradiated TA muscles of immunocompetent mice without any immunosuppressant. Therefore, in our experimental

conditions, the intrinsic function of SM/C-2.6$^+$ satellite cells may be underestimated.

The use of the Lentiviral vector is feasible for ex vivo *gene transfer*: In this study we showed that, at a MOI of 200, lentiviral vectors can introduce the rod-truncated micro-dystrophin gene *CS1* into more than 97% of *mdx*-satellite cells without detrimental effects on cell viability and regenerative capacity. But at a MOI of 300 we observed cell toxicity, whereas at a MOI of 100, the transduction efficiency was below 80% (data not shown). When we injected the transduced autologous myoblasts into *mdx* muscle, the cells contributed to regeneration of myofibers and expressed micro-dystrophin and dystrophin-associated proteins at the sarcolemma. Our results therefore suggest that *ex vivo* gene transfer into autologous myogenic cells by a lentiviral vector is feasible. On the other hand, direct intramuscular injection of vesicular stomatitis virus-G glycoprotein–pseudotyped lentiviral vectors led to relatively low expression of the transgene in mouse skeletal muscles.[30,44] Because the lentiviral vector genome is inserted into the host genome, the transduction of cells other than the target cell could introduce the risk of mutagenesis. Further, *in vivo* administration could induce undesirable immune responses to exogenous viral proteins. In effect, direct *in vivo* administration of lentiviral vectors poses a safety problem for clinical application. In contrast, *ex vivo* gene transfer has the merit of minimizing the risks of introducing free lentiviral vectors into the host. Transduced cells can efficiently proliferate and differentiate *invitro* (data not shown).

Limitations of ex vivo *gene therapy in DMD, using satellite cells*: One of the demerits of our procedure, as compared to *in vivo* gene transfer, is that only a part of the genetically modified myogenic precursor cells contributes to regeneration of the host muscle, given the poor survival rate of these cells. In fact, by using real-time polymerase chain reaction on transcripts from the transgenic enhanced GFP gene, we found that more than 90% of the injected cells were lost within the first 24 hours after injection (data not shown). In addition, migration of the surviving cells is limited in the host muscle after injection. Furthermore, because *in vitro* passaging greatly reduces their myogenicity, it is difficult to obtain a sufficient number of satellite cells or their progeny from a small muscle biopsy of a DMD patient. Therefore current myoblast transfer might be more realistic for localized forms of muscular dystrophy, such as oculo-pharyngeal muscular dystrophy or facio-scapulo-humeral muscular dystrophy.[45] Surprisingly, however, Collins *et al.* transplanted a single intact myofiber into irradiation-ablated muscles and demonstrated that as few as seven satellite cells associated with one transplanted myofiber can generate over 100 new myofibers containing thousands of myonuclei.[5] Their observations suggest that proper isolation and handling of satellite cells might greatly improve their myogenic potential.

In this study we have demonstrated transplantation of autologous satellite cells genetically corrected by a lentiviral vector *ex vivo* into *mdx* muscle. For treating DMD patients, however, it is necessary to find the optimum *in vitro* culture condition that will enable human muscle precursor cells to maintain their intrinsic myogenic potential. It would also be useful to identify the factors that support survival and/or proliferation of transplanted cells in the host muscle.

MATERIALS AND METHODS

Animals. All procedures used on the experimental animals were approved by the Experimental Animal Care and Use Committee at the National Institute of Neuroscience. Eight-to-twelve-week-old C57BL/6 mice were purchased from Nihon CLEA (Tokyo, Japan). C57BL/6-GFP Tg mice were kindly provided by Dr. Okabe (Osaka University, Japan). C57BL/10 mice and C57BL/10-*mdx* mice were maintained in our animal facility and propagated by allowing mating.

In order to induce muscle regeneration, 50 µl of CTX (10 µmol/l in saline; Wako Pure Chemical Industries, Tokyo, Japan) was injected into the TA muscle 24 hours before cell transplantation.

Cell preparation and FACS analysis. Freshly isolated muscle-derived cells were prepared from 8–12-week-old GFP-Tg mice, C57BL/6 mice, C57BL/10 mice, or 5-week-old *mdx* mice as previously described.[35] Hind-limb and fore-limb muscles were isolated and digested with 0.2% type II collagenase (Worthington Biochemical, Lakewood, NJ) for 90 minutes at 37 °C. The muscle slurries were filtered through 100 µm nitrex mesh (BD Biosciences, Franklin Lakes, NJ) and subsequently through 40 µm nitrex mesh (BD Biosciences, Franklin Lakes, NJ). Erythrocytes were eliminated by treatment with 0.8% NH_4Cl in Tris-buffer. Mononucleated cells were stained with biotinylated SM/C-2.6 monoclonal antibody,[35] and labeled by allophycocyanin-conjugated streptavidin (BD PharMingen, San Diego, CA). Mononucleated cells derived from *mdx* muscles were stained with antibodies to additional surface markers, phycoerythrin-conjugated anti-CD45 antibody (clone 30-F11; BD PharMingen, San Diego, CA), phycoerythrin-conjugated anti-CD31 antibody (clone 390; BD PharMingen, San Diego, CA), and phycoerythrin-conjugated anti-Sca-1 antibody (clone D7; BD PharMingen, San Diego, CA). After being washed, stained cells were re-suspended in phosphate-buffered saline (PBS) containing 2% fetal bovine serum (Trace Biosciences, New South Wales, Australia) and 2 µg/ml propidium iodide (BD PharMingen, San Diego, CA). Cell sorting was performed on a FACS VantageSE flow cytometer (BD Biosciences, Franklin Lakes, NJ). Debris and dead cells were excluded by forward scatter, side scatter, and propidium iodide gating. We used only propidium iodide-negative fractions for further experiments. We usually obtained approximately 1.5×10^5 sorted cells from 1 g of muscle of 8–12-week-old female C57BL/6 mice.

Cell culture and intramuscular transplantation. Freshly isolated SM/C-2.6$^+$ cells from GFP-Tg mice were seeded at a density of 1×10^5 cells per 35-mm dish coated with Matrigel (BD Biosciences, Franklin Lakes, NJ) in a growth medium, Dulbecco's modified Eagle's medium (Invitrogen, Carlsbad, CA) containing 20% fetal bovine serum and 2.5 ng/ml basic fibroblast growth factor (Invitrogen, Carlsbad, CA), and expanded for 4 days. Further, these cells were passaged up to three times at 2-day intervals. Primary myoblasts isolated by the pre-plating method[39] from GFP-Tg mice were also cultured in growth medium. Freshly sorted cells, expanded and passaged cells, or cultured primary myoblasts were injected into TA muscles of 8–12-week-old CTX-treated C57BL/6 mice or 5-week-old *mdx* mice that show active cycles of the degeneration–regeneration process. The number of injected cells was 2×10^4 per TA muscle. Four weeks later, the injected muscles were isolated and fixed in 4% paraformaldehyde for 30 minutes, immersed sequentially in 10% sucrose/PBS and 20% sucrose/PBS, and frozen in isopentane cooled with liquid nitrogen.

Immunohistochemistry. Frozen muscle tissues were sectioned (6 µm) using a cryostat. The sections were blocked with 5% goat serum (Cedarlane, Hornby, Canada) in PBS and then reacted with anti-GFP antibody (1:100; Chemicon International, Temecula, CA) and/or anti-laminin $\alpha 2$ antibody (1:100; Alexis, San Diego, CA), or anti-$\alpha 1$-syntrophin antibody

(1:500)[46] at 4 °C overnight. Dystrophin (1:20; NCL-DYSB or DYS2; Novocastra, Newcastle, UK), α-SG (1:50; NCL-α-SARC; Novocastra, Newcastle, UK), and β-dystroglycan (1:50; NCL-β-DG; Novocastra, Newcastle, UK) were detected using monoclonal antibodies after blocking with a MOM kit (Vector Laboratories, Burlingame, CA). The sections were incubated with appropriate combinations of Alexa 488-, Alexa 568-, and Alexa 594-labeled secondary antibodies (Molecular Probes, Eugene, OR) for 30 minutes. The nuclei were counterstained with TOTO-3 (1:5,000; Molecular Probes, Eugene, OR). The stained sections were observed under the confocal laser scanning microscope system TCSSP (Leica, Heidelberg, Germany).

Immunocytochemistry. Cells sorted using FACS were collected by Cytospin3 (Thermo Fisher Scientific, Waltham, MA). After being fixed with 4% paraformaldehyde for 10 minutes, the cells were blocked with 5% goat serum in PBS and then reacted with anti-Pax7 antibody (1:2; Developmental Studies Hybridoma Bank, Iowa, IA), anti-MyoD antibody (1:200; Dako, Glostrup, Denmark), anti-myogenin antibody (1:200; Developmental Studies Hybridoma Bank, Iowa, IA), and anti-Ki67 antibody (1:2, Ylem, Rome, Italy) at 4 °C overnight. Primary antibodies were detected by Alexa 488- or Alexa 568-labeled secondary antibodies (Molecular Probes, Eugene, OR) for 30 minutes. Stained cells were mounted in Vectashield with 4′,6-diamidino-2-phenylindole (Vector Laboratories, Burlingame, CA) and observed with fluorescence microscopy IX70 (Olympus, Tokyo, Japan).

Generation of lentiviral vectors and* in vitro *transduction. The third-generation self-inactivated human immunodeficiency virus-1-based lentiviral vector, pCSII-CMV-IRES2-Venus, has been described previously.[47] The vector contains a CMV promoter; an internal ribosomal entry site (IRES) followed by *Venus*, which is a variant of yellow fluorescent protein[41]; and a woodchuck hepatitis virus post-transcriptional regulatory element. A rod-truncated micro-dystrophin *CS1* complementary DNA (four rod repeats, 4.9 kb) was excised from pCAG-*CS1*[24] and cloned into pCSII-CMV-IRES2-Venus, generating pCSII-CMV-*CS1*-IRES2-Venus. The lentiviral vectors expressing Venus only, or micro-dystrophin *CS1* followed by Venus, were generated by transient cotransfection of the pCSII-CMV-IRES2-Venus or pCSII-CMV-*CS1*-IRES2-Venus, respectively, with the packaging construct (pCAG-HIVgp), vesicular stomatitis virus-G protein, and Rev-expressing construct (pCMV-VSV-G-RSV-Rev) into 293T cells, using the calcium phosphate transfection method.[47–49] Two days after transfection, the vector-containing supernatant was collected, filtered through a 0.45-μm-pore-size filter (Thermo Fisher Scientific, Waltham, MA), and concentrated by centrifugation twice at 50,000*g* for 2 hours at 20 °C. The virus pellet was re-suspended in Hank's Balanced Salt Solution (Invitrogen, Carlsbad, CA) and stored at −80 °C until use. The titer of the concentrated virus was 5×10^8 to 1×10^9 infectious units/ml when assayed on 293T cells, and infectivity was determined by Venus expression as analyzed on a FACS VantageSE (BD Biosciences, Franklin Lakes, NJ).

Sixty thousand freshly isolated SM/C-2.6$^+$ cells in 300 μl growth medium were seeded in each well of 24-well plates and cultured for 16 hours with viral vectors expressing Venus or micro-dystrophin *CS1* at MOI of 100 or 200, respectively. After removal of free viral vectors by changing the medium, the transduced cells were cultured for 2 or 3 days and trypsinized. A cell suspension containing 2×10^1 cells in 20 μl of PBS was injected into the TA muscles of *mdx* mice. The infection efficiency of the injected cells was evaluated using a FACS VantageSE (BD Biosciences, Franklin Lakes, NJ).

ACKNOWLEDGMENTS

This work was supported by Research on Nervous and Mental Disorders (16B-2), and Health Science Research Grants for Research on the Human Genome and Gene Therapy (H16-genome-003), for Research on Brain Science (H15-kokoro-021, H18-kokoro-019) from the Japanese Ministry of Health, Labor and Welfare, Grants-in-Aids for Scientific Research (14657158, 15390281, 16590333, and 18590392) from the Japanese Ministry of Education, Culture, Sports, Science and Technology, and the "Ground-based Research Program for Space Utilization" promoted by the Japan Space Forum.

SUPPLEMENTARY MATERIAL

Figure S1. Freshly isolated satellite cells give rise to larger colonies than passaged myoblasts *in vitro*.

REFERENCES

1. Emery, AE (1993). Duchenne muscular dystrophy—Meryon's disease. *Neuromuscul Disord* **3**: 263–266.
2. Ervasti, JM and Campbell, KP (1993). A role for the dystrophin-glycoprotein complex as a transmembrane linker between laminin and actin. *J Cell Biol* **122**: 809–823.
3. Suzuki, A, Yoshida, M, Hayashi, K, Mizuno, Y, Hagiwara, Y and Ozawa, E (1994). Molecular organization at the glycoprotein-complex-binding site of dystrophin. Three dystrophin-associated proteins bind directly to the carboxy-terminal portion of dystrophin. *Eur J Biochem* **220**: 283–292.
4. Charge, SB and Rudnicki, MA (2004). Cellular and molecular regulation of muscle regeneration. *Physiol Rev* **84**: 209–238.
5. Collins, CA, Olsen, I, Zammit, PS, Heslop, L, Petrie, A, Partridge, TA *et al.* (2005). Stem cell function, self-renewal, and behavioral heterogeneity of cells from the adult muscle satellite cell niche. *Cell* **122**: 289–301.
6. Schultz, E (1996). Satellite cell proliferative compartments in growing skeletal muscles. *Dev Biol* **175**: 84–94.
7. Kinoshita, I, Vilquin, JT, Guerette, B, Asselin, I, Roy, R and Tremblay, JP (1994). Very efficient myoblast allotransplantation in mice under FK506 immunosuppression. *Muscle Nerve* **17**: 1407–1415.
8. Skuk, D, Roy, B, Goulet, M, Chapdelaine, P, Bouchard, JP, Roy, R *et al.* (2004). Dystrophin expression in myofibers of Duchenne muscular dystrophy patients following intramuscular injections of normal myogenic cells. *Mol Ther* **9**: 475–482.
9. Gussoni, E, Pavlath, GK, Lanctot, AM, Sharma, KR, Miller, RG, Steinman, L *et al.* (1992). Normal dystrophin transcripts detected in Duchenne muscular dystrophy patients after myoblast transplantation. *Nature* **356**: 435–438.
10. Mendell, JR, Kissel, JT, Amato, AA, King, W, Signore, L, Prior, TW *et al.* (1995). Myoblast transfer in the treatment of Duchenne's muscular dystrophy. *N Engl J Med* **333**: 832–838.
11. Gussoni, E, Blau, HM and Kunkel, LM (1997). The fate of individual myoblasts after transplantation into muscles of DMD patients. *Nat Med* **3**: 970–977.
12. Beauchamp, JR, Morgan, JE, Pagel, CN and Partridge, TA (1999). Dynamics of myoblast transplantation reveal a discrete minority of precursors with stem cell-like properties as the myogenic source. *J Cell Biol* **144**: 1113–1122.
13. Hodgetts, SI, Beilharz, MW, Scalzo, AA and Grounds, MD (2000). Why do cultured transplanted myoblasts die *in vivo*? DNA quantification shows enhanced survival of donor male myoblasts in host mice depleted of CD4+ and CD8+ cells or Nk1.1+ cells. *Cell Transplant* **9**: 489–502.
14. Skuk, D, Caron, NJ, Goulet, M, Roy, B and Tremblay, JP (2003). Resetting the problem of cell death following muscle-derived cell transplantation: detection, dynamics and mechanisms. *J Neuropathol Exp Neurol* **62**: 951–967.
15. Skuk, D, Goulet, M, Roy, B and Tremblay, JP (2002). Efficacy of myoblast transplantation in nonhuman primates following simple intramuscular cell injections: toward defining strategies applicable to humans. *Exp Neurol* **175**: 112–126.
16. Skuk, D, Goulet, M, Roy, B, Chapdelaine, P, Bouchard, JP, Roy, R *et al.* (2006). Dystrophin expression in muscles of duchenne muscular dystrophy patients after high-density injections of normal myogenic cells. *J Neuropathol Exp Neurol* **65**: 371–386.
17. Skuk, D, Goulet, M, Roy, B, Piette, V, Cote, CH, Chapdelaine, P *et al.* (2007). First test of a "high-density injection" protocol for myogenic cell transplantation throughout large volumes of muscles in a Duchenne muscular dystrophy patient: eighteen months follow-up. *Neuromuscul Disord* **17**: 38–46.
18. Morgan, JE, Pagel, CN, Sherratt, T and Partridge, TA (1993). Long-term persistence and migration of myogenic cells injected into pre-irradiated muscles of mdx mice. *J Neurol Sci* **115**: 191–200.
19. Morgan, JE, Fletcher, RM and Partridge, TA (1996). Yields of muscle from myogenic cells implanted into young and old mdx hosts. *Muscle Nerve* **19**: 132–139.
20. Mueller, GM, O'Day, T, Watchko, JF and Ontell, M (2002). Effect of injecting primary myoblasts versus putative muscle-derived stem cells on mass and force generation in mdx mice. *Hum Gene Ther* **13**: 1081–1090.
21. Praud, C, Montarras, D, Pinset, C and Sebille, A (2003). Dose effect relationship between the number of normal progenitor muscle cells grafted in mdx mouse skeletal striated muscle and the number of dystrophin-positive fibres. *Neurosci Lett* **352**: 70–72.
22. Qu-Petersen, Z, Deasy, B, Jankowski, R, Ikezawa, M, Cummins, J, Pruchnic, R *et al.* (2002). Identification of a novel population of muscle stem cells in mice: potential for muscle regeneration. *J Cell Biol* **157**: 851–864.
23. Montarras, D, Morgan, J, Collins, C, Relaix, F, Zaffran, S, Cumano, A *et al.* (2005). Direct isolation of satellite cells for skeletal muscle regeneration. *Science* **309**: 2064–2067.
24. Sakamoto, M, Yuasa, K, Yoshimura, M, Yokota, T, Ikemoto, T, Suzuki, M *et al.* (2002). Micro-dystrophin cDNA ameliorates dystrophic phenotypes when introduced into mdx mice as a transgene. *Biochem Biophys Res Commun* **293**: 1265–1272.
25. Yoshimura, M, Sakamoto, M, Ikemoto, M, Mochizuki, Y, Yuasa, K, Miyagoe-Suzuki, Y *et al.* (2004). AAV vector-mediated microdystrophin expression in a relatively

small percentage of mdx myofibers improved the mdx phenotype. *Mol Ther* **10**: 821–828.
26. Fabb, SA, Wells, DJ, Serpente, P and Dickson, G (2002). Adeno-associated virus vector gene transfer and sarcolemmal expression of a 144 kDa micro-dystrophin effectively restores the dystrophin-associated protein complex and inhibits myofibre degeneration in nude/mdx mice. *Hum Mol Genet* **11**: 733–741.
27. Harper, SQ, Hauser, MA, DelloRusso, C, Duan, D, Crawford, RW, Phelps, SF *et al.* (2002). Modular flexibility of dystrophin: implications for gene therapy of Duchenne muscular dystrophy. *Nat Med* **8**: 253–261.
28. Acsadi, G, Dickson, G, Love, DR, Jani, A, Walsh, FS, Gurusinghe, A *et al.* (1991). Human dystrophin expression in mdx mice after intramuscular injection of DNA constructs. *Nature* **352**: 815–818.
29. Quenneville, SP, Chapdelaine, P, Rousseau, J, Beaulieu, J, Caron, NJ, Skuk, D *et al.* (2004). Nucleofection of muscle-derived stem cells and myoblasts with phiC31 integrase: stable expression of a full-length-dystrophin fusion gene by human myoblasts. *Mol Ther* **10**: 679–687.
30. Li, S, Kimura, E, Fall, BM, Reyes, M, Angello, JC, Welikson, R *et al.* (2005). Stable transduction of myogenic cells with lentiviral vectors expressing a minidystrophin. *Gene Ther* **12**: 1099–1108.
31. Quenneville, SP, Chapdelaine, P, Skuk, D, Paradis, M, Goulet, M, Rousseau, J *et al.* (2007). Autologous transplantation of muscle precursor cells modified with a lentivirus for muscular dystrophy: human cells and primate models. *Mol Ther* **15**: 431–438.
32. Bachrach, E, Li, S, Perez, AL, Schienda, J, Liadaki, K, Volinski, J *et al.* (2004). Systemic delivery of human microdystrophin to regenerating mouse dystrophic muscle by muscle progenitor cells. *Proc Natl Acad Sci USA* **101**: 3581–3586.
33. Sampaolesi, M, Torrente, Y, Innocenzi, A, Tonlorenzi, R, D'Antona, G, Pellegrino, MA *et al.* (2003). Cell therapy of alpha-sarcoglycan null dystrophic mice through intra-arterial delivery of mesoangioblasts. *Science* **301**: 487–492.
34. Sampaolesi, M, Blot, S, D'Antona, G, Granger, N, Tonlorenzi, R, Innocenzi, A *et al.* (2006). Mesoangioblast stem cells ameliorate muscle function in dystrophic dogs. *Nature* **444**: 574–579.
35. Fukada, S, Higuchi, S, Segawa, M, Koda, K, Yamamoto, Y, Tsujikawa, K *et al.* (2004). Purification and cell-surface marker characterization of quiescent satellite cells from murine skeletal muscle by a novel monoclonal antibody. *Exp Cell Res* **296**: 245–255.
36. Zammit, PS, Golding, JP, Nagata, Y, Hudon, V, Partridge, TA and Beauchamp, JR (2004). Muscle satellite cells adopt divergent fates: a mechanism for self-renewal? *J Cell Biol* **166**: 347–357.
37. Yablonka-Reuveni, Z and Rivera, AJ (1994). Temporal expression of regulatory and structural muscle proteins during myogenesis of satellite cells on isolated adult rat fibers. *Dev Biol* **164**: 588–603.
38. Cornelison, DD and Wold, BJ (1997). Single-cell analysis of regulatory gene expression in quiescent and activated mouse skeletal muscle satellite cells. *Dev Biol* **191**: 270–283.
39. Rando, TA and Blau, HM (1994). Primary mouse myoblast purification, characterization, and transplantation for cell-mediated gene therapy. *J Cell Biol* **125**: 1275–1287.
40. Burns, JC, Friedmann, T, Driever, W, Burrascano, M and Yee, JK (1993). Vesicular stomatitis virus G glycoprotein pseudotyped retroviral vectors: concentration to very high titer and efficient gene transfer into mammalian and nonmammalian cells. *Proc Natl Acad Sci USA* **90**: 8033–8037.
41. Nagai, T, Ibata, K, Park, ES, Kubota, M, Mikoshiba, K and Miyawaki, A (2002). A variant of yellow fluorescent protein with fast and efficient maturation for cell-biological applications. *Nat Biotechnol* **20**: 87–90.
42. Smythe, GM, Hodgetts, SI and Grounds, MD (2001). Problems and solutions in myoblast transfer therapy. *J Cell Mol Med* **5**: 33–47.
43. Hashimoto, N, Murase, T, Kondo, S, Okuda, A and Inagawa-Ogashiwa, M (2004). Muscle reconstitution by muscle satellite cell descendants with stem cell-like properties. *Development* **131**: 5481–5490.
44. Kobinger, GP, Louboutin, JP, Barton, ER, Sweeney, HL and Wilson, JM (2003). Correction of the dystrophic phenotype by *in vivo* targeting of muscle progenitor cells. *Hum Gene Ther* **14**: 1441–1449.
45. Mouly, V, Aamiri, A, Perie, S, Mamchaoui, K, Barani, A, Bigot, A *et al.* (2005). Myoblast transfer therapy: is there any light at the end of the tunnel? *Acta Myol* **24**: 128–133.
46. Kameya, S, Miyagoe, Y, Nonaka, I, Ikemoto, T, Endo, M, Hanaoka, K *et al.* (1999). Alpha1-syntrophin gene disruption results in the absence of neuronal-type nitric-oxide synthase at the sarcolemma but does not induce muscle degeneration. *J Biol Chem* **274**: 2193–2200.
47. Miyoshi, H, Blomer, U, Takahashi, M, Gage, FH and Verma, IM (1998). Development of a self-inactivating lentivirus vector. *J Virol* **72**: 8150–8157.
48. Naldini, L, Blomer, U, Gallay, P, Ory, D, Mulligan, R, Gage, FH *et al.* (1996). *In vivo* gene delivery and stable transduction of nondividing cells by a lentiviral vector. *Science* **272**: 263–267.
49. Dull, T, Zufferey, R, Kelly, M, Mandel, RJ, Nguyen, M, Trono, D *et al.* (1998). A third-generation lentivirus vector with a conditional packaging system. *J Virol* **72**: 8463–8471.

STEM CELLS
TISSUE-SPECIFIC STEM CELLS

Molecular Signature of Quiescent Satellite Cells in Adult Skeletal Muscle

SO-ICHIRO FUKADA,[a] AKIYOSHI UEZUMI,[a] MADOKA IKEMOTO,[a] SATORU MASUDA,[a] MASASHI SEGAWA,[b] NAOKI TANIMURA,[c] HIROSHI YAMAMOTO,[b] YUKO MIYAGOE-SUZUKI,[a] SHIN'ICHI TAKEDA[a]

[a]Department of Molecular Therapy, National Institute of Neuroscience, National Center of Neurology and Psychiatry, Tokyo, Japan; [b]Department of Immunology, Graduate School of Pharmaceutical Sciences, Osaka University, Osaka, Japan; [c]Bio and Nano Technologies, Science and Technology Division, Mizuho Information & Research Institute Inc., Tokyo, Japan

Key Words. Fluorescence-activated cell sorting • Microarray • Quiescence • Muscle satellite cells • Calcitonin receptor

ABSTRACT

Skeletal muscle satellite cells play key roles in postnatal muscle growth and regeneration. To study molecular regulation of satellite cells, we directly prepared satellite cells from 8- to 12-week-old C57BL/6 mice and performed genome-wide gene expression analysis. Compared with activated/cycling satellite cells, 507 genes were highly upregulated in quiescent satellite cells. These included negative regulators of cell cycle and myogenic inhibitors. Gene set enrichment analysis revealed that quiescent satellite cells preferentially express the genes involved in cell-cell adhesion, regulation of cell growth, formation of extracellular matrix, copper and iron homeostasis, and lipid transportation. Furthermore, reverse transcription-polymerase chain reaction on differentially expressed genes confirmed that calcitonin receptor (CTR) was exclusively expressed in dormant satellite cells but not in activated satellite cells. In addition, CTR mRNA is hardly detected in nonmyogenic cells. Therefore, we next examined the expression of CTR in vivo. CTR was specifically expressed on quiescent satellite cells, but the expression was not found on activated/proliferating satellite cells during muscle regeneration. CTR-positive cells reappeared at the rim of regenerating myofibers in later stages of muscle regeneration. Calcitonin stimulation delayed the activation of quiescent satellite cells. Our data provide roles of CTR in quiescent satellite cells and a solid scaffold to further dissect molecular regulation of satellite cells. STEM CELLS *2007;25:2448–2459*

Disclosure of potential conflicts of interest is found at the end of this article.

INTRODUCTION

Muscle satellite cells, which account for 2%–5% of the total nuclei in adult skeletal muscle, play a major role in muscle regeneration [1, 2]. Under normal conditions, satellite cells are found external to the myofiber plasma membrane and beneath the muscle basal lamina [3] and are mitotically quiescent in the adult skeletal muscle [4, 5]. When activated by muscle damage, they proliferate, differentiate, fuse with each other or injured fibers, and eventually regenerate mature myofibers under the influence of innervation [6]. Recently, it was clearly demonstrated that the proliferation capacity of satellite cells in vivo is robust and that the contribution of interstitial cells or bone marrow-derived cells to muscle fiber regeneration is limited [7]. Importantly, a small fraction of activated satellite cells exit the cell cycle and return to the quiescent satellite state during muscle regeneration to maintain their numbers and the regenerative capacity of muscle.

Besides muscle fiber repair, satellite cells are also responsible for postnatal growth [8] and hypertrophy of skeletal muscle [9], and impairment of their functions is related to several pathological conditions, for example, muscular dystrophies and aging-related muscle atrophy [10]. Moreover, several studies showed that satellite cells differentiate into adipogenic cells or osteocytes in vitro [11–13], implying that they contribute to the fatty infiltration seen in Duchenne muscular dystrophy. Thus, normal functioning of satellite cells is indispensable for the integrity of skeletal muscle, and the cells themselves are an important source of cells for cell therapy of muscle diseases, making it valuable to clarify the molecular regulation of maintenance, activation/proliferation, and differentiation in satellite cells.

Like hematopoietic stem cells, most satellite cells are in a quiescent and undifferentiated state in the adult. Although quiescence is important to retain the proliferative and differentiative potential of satellite cells throughout the lifetime, the molecular regulation of quiescence remains poorly defined. Recent studies suggested that myostatin, a skeletal muscle-specific transforming growth factor-β superfamily member, suppresses the activation of satellite cells [14]. Myostatin has been shown to induce a potent cyclin-dependent kinase inhibitor, p21(Cdkn1a), in vitro [15]. Other in vitro studies suggested that the decrease of MyoD protein and induction of another cyclin-dependent kinase inhibitor, p27(Cdkn1b) [16], and a Rb-related pocket protein, p130 [16, 17], are involved in the attainment of quiescence by proliferating myoblasts.

Correspondence: Yuko Miyagoe-Suzuki, M.D., Ph.D., Department of Molecular Therapy, National Institute of Neuroscience, National Center of Neurology and Psychiatry, 4-1-1 Ogawa-higashi, Kodaira, Tokyo 187-8502, Japan. Telephone: +81-42-346-1720; Fax: +81-42-346-1750; e-mail: miyagoe@ncnp.go.jp Received January 8, 2007; accepted for publication June 19, 2007; first published online in STEM CELLS *EXPRESS* June 28, 2007. 1066-5099/2007/$30.00/0 doi: 10.1634/stemcells.2007-0019

We previously reported a method to purify quiescent satellite cells from adult skeletal muscle using the fluorescence-activated cell sorting (FACS) technique and a novel antibody named SM/C-2.6 [18]. In this study, to clarify the molecular regulation of quiescent satellite cells, we performed genome-wide gene expression profiling of quiescent satellite cells isolated from C57BL/6 mice. Expression analysis of individual genes identified several candidate genes that regulate dormancy of satellite cells. Gene set enrichment analysis (GSEA) revealed that the gene sets involved in cell-cell adhesion, cell growth, copper and iron ion homeostasis, lipid transport, and formation of extracellular matrix were coordinately upregulated in quiescent satellite cells. Furthermore, we demonstrate that calcitonin receptor (CTR) is expressed specifically on quiescent satellite cells in vivo and that calcitonin significantly attenuates the activation of satellite cells. Our study is the first report of in-depth gene expression analysis of quiescent satellite cells and will greatly facilitate the investigation of molecular regulation of satellite cells in both physiological and pathological conditions.

MATERIALS AND METHODS

Animals

All procedures using experimental animals were approved by the Experimental Animal Care and Use Committee at the National Institute of Neuroscience. C57BL/6 mice were purchased from Nihon CLEA (Tokyo, http://www.clea-japan.com).

Preparation of Satellite Cells and Nonmyogenic Cells from Mouse Limb Muscles

Mononuclear cells were prepared from fore- and hindlimb muscles of 8- to 12-week-old female C57BL/6 mice as described [19] and incubated on ice for 30 minutes in the presence of a 1:200 dilution of phycoerythrin-conjugated anti-CD45 (clone: 30-F11) and biotinylated SM/C-2.6 [18]. Cells were then incubated with streptavidin-labeled allophycocyanin on ice for 30 minutes and resuspended in phosphate-buffered saline (PBS) containing 2% fetal bovine serum (FBS) and 2 μg/ml propidium iodide (PI). Cell sorting was performed on a FACSVantage SE flow cytometer (BD Biosciences, San Diego, http://www.bdbiosciences.com). Dead cells were excluded by PI gating. All antibodies and reagents for FACS analysis were purchased from BD Pharmingen (San Diego, http://www.bdbiosciences.com/index_us.shtml).

Cell Culture

Satellite cells were cultured in growth medium consisting of high-glucose Dulbecco's modified Eagle's medium (DMEM; Invitrogen, Carlsbad, CA, http://www.invitrogen.com) containing 20% fetal calf serum (FCS; Trace Biosciences, New South Wales, Australia), 2.5 ng/ml basic fibroblast growth factor (Invitrogen), and penicillin (100 U/ml)-streptomycin (100 μg/ml) (Gibco-BRL, Gaithersburg, MD, http://www.gibcobrl.com) on culture dishes coated with Matrigel (BD Biosciences). Single living myofibers were prepared as described [20] and transferred to Matrigel-coated 24-well culture dishes (one fiber per well). After a 2-day culture in growth medium with or without elcatonin, satellite cells that had detached from muscle fibers were counted.

Immunocytochemical Analysis

FACS-sorted cells were collected on glass slides by Cytospin 3 (Thermo Shandon Inc., Pittsburgh, http://www.thermo.com) and immunostained as described [19]. Cultured cells were fixed on 8-well Lab-Tek Chamber Slides (Nunc, Rochester, NY, http://www.nuncbrand.com) and stained as described [19, 21] with mouse anti-Pax7 (1:100; clone: Pax7; Developmental Studies Hybridoma Bank, Iowa City, IA, http://www.uiowa.edu/~dshbwww), mouse anti-MyoD (1:200; clone: 5.8A; NeoMarkers; Lab Vision, Fremont, CA, http://www.labvision.com), mouse anti-myogenin (1:100; clone: F5D; Developmental Studies Hybridoma Bank), rabbit anti-Ki67 (1:2; Ylem, Rome), or rabbit anti-p57 antibodies (1:50; GeneTex, San Antonio, http://www.genetex.com) at 4°C overnight and then reacted with secondary antibodies conjugated with Alexa 488 or Alexa 568 (Molecular Probes, Eugene, OR, http://probes.invitrogen.com). Nuclei were stained with 4,6-diamidino-2-phenylindole (DAPI). Images were photographed using a phase-contrast and fluorescence microscope IX70 (Olympus, Tokyo, http://www.olympus-global.com) equipped with a Quantix air-cooled CCD camera (Photometrics, Kew, VIC, Australia, http://www.photometrix.com.au) and IP Lab software (Scanalytics, Rockville, MD, http://www.scanalytics.com).

Immunohistochemistry

Immunostaining of muscle cryosections was performed as previously described [21] using rat anti-laminin α2 (1:200; clone 4H8-2; Alexis Biochemical, Lausen, Switzerland, http://www.axxora.com), rabbit anti-M-cadherin [21], rabbit anti-human CTR (1:200; Serotec Ltd., Oxford, U.K., http://www.serotec.com), goat anti-Notch 3 (1:100; R&D Systems Inc., Minneapolis, http://www.rndsystems.com), or mouse anti-Pax7. Rabbit anti-mouse HeyL polyclonal antibody was produced in our laboratory. In brief, the DNA fragment corresponding to amino acids 220–287 of mouse HeyL (GenBank: NM_013905) was fused to glutathione *S*-transferase in the pGEX-1 Lambda T vector (GE Healthcare, Uppsala, Sweden, http://www.gehealthcare.com). The purified fusion protein was used to immunize New Zealand White rabbits. The obtained serum was affinity-purified. For Pax7 staining, an M.O.M. kit (Vector Laboratories, Burlingame, CA, http://www.vectorlabs.com) was used to block endogenous mouse IgG. For CTR staining, horseradish peroxidase-conjugated anti-rabbit IgG donkey secondary antibody (1:100; GE Healthcare) and Alexa 568-conjugated Tyramid (Molecular Probes) were used to amplify the signal. Nuclei were counterstained with TOTO-3 (1:5,000; Molecular Probes) or DAPI. The images were recorded using a confocal laser scanning microscope system TCSSP (Leica, Heerbrugg, Switzerland, http://www.leica.com) or Axiophot microscope (Carl Zeiss, Jena, Germany, http://www.zeiss.com).

Cell Cycle Analysis

Muscle-derived mononucleated cells or cultured SM/C-2.6 positive cells were suspended at 10^6 cells per milliliter in DMEM (Invitrogen) containing 2% FBS (Trace Biosciences), 10 mM Hepes, and 10 μM Hoechst 33342 (Sigma-Aldrich, St. Louis, http://www.sigmaaldrich.com) and incubated for 45 minutes at 37°C. An additional incubation was performed in the presence of 10 μg/ml Pyronin Y (Sigma-Aldrich) for 45 minutes at 37°C. Cells were then washed with PBS containing 2% FCS. Muscle-derived mononucleated cells were stained with SM/C-2.6 antibody and analyzed by FACSVantage SE flow cytometer.

Cell Proliferation Assay

After cell sorting, quiescent satellite cells were plated on 96-well culture plates at a density of 3,000–8,000 in the absence or presence of elcatonin (0.01–0.1 U/ml) (Asahi Kasei Pharma Corporation, Tokyo, http://www.asahi-kasei.co.jp/asahi/en) and cultured for 1–2 days. Then 5-bromo-2′-deoxyuridine (BrdU) (10 μM) was added to the culture. To examine the effects of elcatonin on activated satellite cells, satellite cells were cultured for 3 days and then elcatonin was added to the culture 24 hours before addition of BrdU. Twenty-four hours later, BrdU uptake was quantified by cell proliferation enzyme-linked immunosorbent assay, BrdU Kit (Roche Diagnostics, Basel, Switzerland, http://www.roche-applied-science.com), and lumi-Image F1 (Roche). In Figure 6B, cells were exposed to elcatonin for 30 minutes and washed twice with PBS and then plated on culture dishes.

Detection of Apoptotic Cells

Cells were cultured on 8-well Lab-Tek chamber slides with or without elcatonin. Apoptotic cells were detected by rhodamine fluorescence using an ApopTag Red In Situ Apoptosis Detection Kit (Chemicon, Temecula, CA, http://www.chemicon.com).

RNA Extraction and Reverse Transcription-Polymerase Chain Reaction

Total RNA was extracted from sorted or cultured cells with a Qiagen RNeasy Mini kit according to the manufacturer's instructions (Qiagen, Hilden, Germany, http://www1.qiagen.com) and then reverse-transcribed into cDNA by using TaqMan Reverse Transcription Reagents (Roche). The polymerase chain reaction (PCR) was performed with cDNA products under the following cycling conditions: 94°C for 3 minutes followed by 30–40 cycles of amplification, annealing, and extension (94°C for 15 seconds, 58°C for 30 seconds, and 72°C for 30 seconds) with a final incubation at 72°C for 5 minutes. Specific primer sequences used for PCR are described in supplemental online Materials and Methods.

Target Synthesis, Gene Chip Hybridization, and Data Acquisition

To label antisense RNA (aRNA) with biotin for microarray hybridization, we followed the protocol supplied by the manufacturer (Affymetrix, Santa Clara, CA, http://www.affymetrix.com). Because the starting amount of total RNA was 100 ng for the sorted SM/C-2.6$^+$ cell fraction, we used a two-cycle biotin aRNA synthesis kit (Affymetrix). Labeled aRNA was fragmented according to Affymetrix GeneChip protocol and then hybridized to Affymetrix MOE430A GeneChip arrays for 16 hours. After washing, the gene chips were stained according to the instrument's standard Eukaryotic GE WS2v4 protocol using antibody-mediated signal amplification. The signal was determined, using the Microarray Suite (MAS) 5.0 absolute analysis algorithm, as the average fluorescence intensity among the intensities obtained from the probe set. The signal of a probe set was calculated as the one-step biweight estimate of combined differences of all the probe pairs (perfectly matched and mismatched) in the probe set. A one-sided Wilcoxon's signed rank test was used to calculate a p value that reflects the significance of differences between perfectly matched and mismatched probe pairs. The p value was used to make the absolute call for probe sets. A "Present" call was assigned to transcripts for p values between 0 and .04, a "Marginal" call was assigned to transcripts for p values between .04 and .06, and an "Absent" call was assigned to transcripts for p values between .06 and 1.0.

Microarray Data Analysis

Scanned output files were analyzed by the probe level analysis package MAS 5.0 (Affymetrix). The Present/Absent call provided by the Affymetrix programs was used for the first selection. The MAS 5.0-generated raw data were uploaded to GeneSpring software version 7.0 (Silicongenetics, Redwood, CA, http://www.chem.agilent.com/scripts/PHome.asp). Data normalization was achieved by one of two methods: (a) each signal was divided by the 50th percentile of all signals in a specific hybridization experiment or (b) each signal was divided by the median of its values in all samples. A more reliable list of "5-fold changing" genes was obtained by applying the filtering options of GeneSpring. Present calls in all (four) quiescent or activated satellite cell probes were selected and a restriction, which passed genes with raw data above 100, was applied. Then, using all the quiescent and activated satellite cells as data, we performed a one-way analysis of variance test between the quiescent satellite cell group and the activated satellite cell group. In particular, a parametric test, with variances assumed equal (Student's t test, p value cut-off .05; multiple testing correction: Benjamini and Hochberg false discovery rate), was applied. The genes passing all these filters and tests were selected as "5-fold changing genes." Nonmyogenic cells (SM/C-2.6$^-$/CD45$^-$ cells) were also prepared four times.

Gene Set Enrichment Analysis

GSEA [22] is a statistical analysis of sets of gene expression profiles, separated by phenotypic labels. Using GSEA, we can test hypotheses concerned with predefined sets of genes; the rank orderings of the genes in the whole gene set calculated with a given ranking method are random with regard to a given classification of samples. As a result of the analysis, nominal p values, family-wise error rate p values, and false discovery rate (FDR) q values for test hypotheses (thus for gene sets) were obtained.

In our analysis, we used the GSEA-P software package [22], which is available from the Broad Institute (Cambridge, MA, http://www.broad.mit.edu). We prepared, as input to the GSEA-P, the MAS 5.0-generated raw signal data and gene sets derived independently. We chose genes on the chip that were detected (the Present call was assigned) in at least one sample (17,150 of 22,626). The raw signals of the chosen genes were normalized so that their total sum was 1. Because the total amount of mRNA in a quiescent satellite cell (QSC) is much less than that in an activated satellite cell (ASC), the normalized signal should be understood as a relative signal among the chosen genes. To compile the gene sets, we assigned each probe to a gene ontology (GO) category [23] using annotations of the MOE430A chip (September 22, 2005) provided by Affymetrix. Therefore, these gene sets reflect the structure of the GO categories and subcategories of molecular function (MF), biological process (BP), and cellular component (CC). The 17,150 genes chosen comprised 1,674, 1,698, and 412 gene sets in the MF, BP, and CC subcategories, respectively, and were reduced to 162, 218, and 85 after filtering out gene sets with sizes smaller than 20 or larger than 1,000. We ran the GSEA-P with the signal-to-noise option for its ranking metric, with permutation over phenotype labels of QSC and ASC samples, and repeated it 2,000 times with the "weighted" option for its scoring scheme.

Results and Discussion

Isolation of Quiescent Satellite Cells from Mouse Skeletal Muscle

First, to obtain RNA samples for microarray analysis, we prepared mononuclear cells from 8- to 12-week-old C57BL/6 mouse muscle, and the SM/C-2.6$^+$ fraction was collected as the satellite cell fraction by FACS [18] (Fig. 1A). Consistent with our previous report, more than 97% of fresh SM/C-2.6$^+$ cells expressed Pax7 (Fig. 1B) but were mostly negative for both MyoD (Fig. 1Ca, 1Cb) and Ki67 (Fig. 1Ce, 1Cf). After 4–5 days of culture, more than 98% of SM/C-2.6$^+$ cells expressed MyoD (Fig. 1Cg, 1Ch) and Ki67 (Fig. 1Ck, 1Cl). Both freshly isolated, uncultured SM/C-2.6$^+$ cells and SM/C-2.6$^+$ cells cultured in growth medium were negative for myogenin expression (Fig. 1Cc, 1Cd, 1Ci, 1Cj), but these cells started to express myogenin and differentiated well into multinucleated myotubes after mitogen withdrawal (data not shown). In contrast, more than 99% of freshly isolated SM/C-2.6$^-$/CD45$^-$ cells were negative for Pax7 expression (Fig. 1Bc, 1Bd), and cultured SM/C-2.6$^-$/CD45$^-$ cells did not express MyoD (data not shown), again indicating that myogenic cells are highly enriched in the SM/C-2.6$^+$ fraction.

The forward and side scatter profiles of freshly isolated SM/C-2.6$^+$ cells showed that they are small and uniform in granularity (data not shown). In fact, as shown in Figure 1D, the cell size of fresh SM/C-2.6$^+$ cells was estimated to be approximately one-half that of cultured SM/C-2.6$^+$ cells based on the forward scatter profile, indicating that the freshly isolated SM/C-2.6$^+$ cells were not activated yet. Pyronin Y staining showed the small amount of RNA content in freshly isolated SM/C-2.6$^+$ cells (Fig. 1D). In general, a Pyronin^{low} and Hoechst 33342^{low} fraction is considered

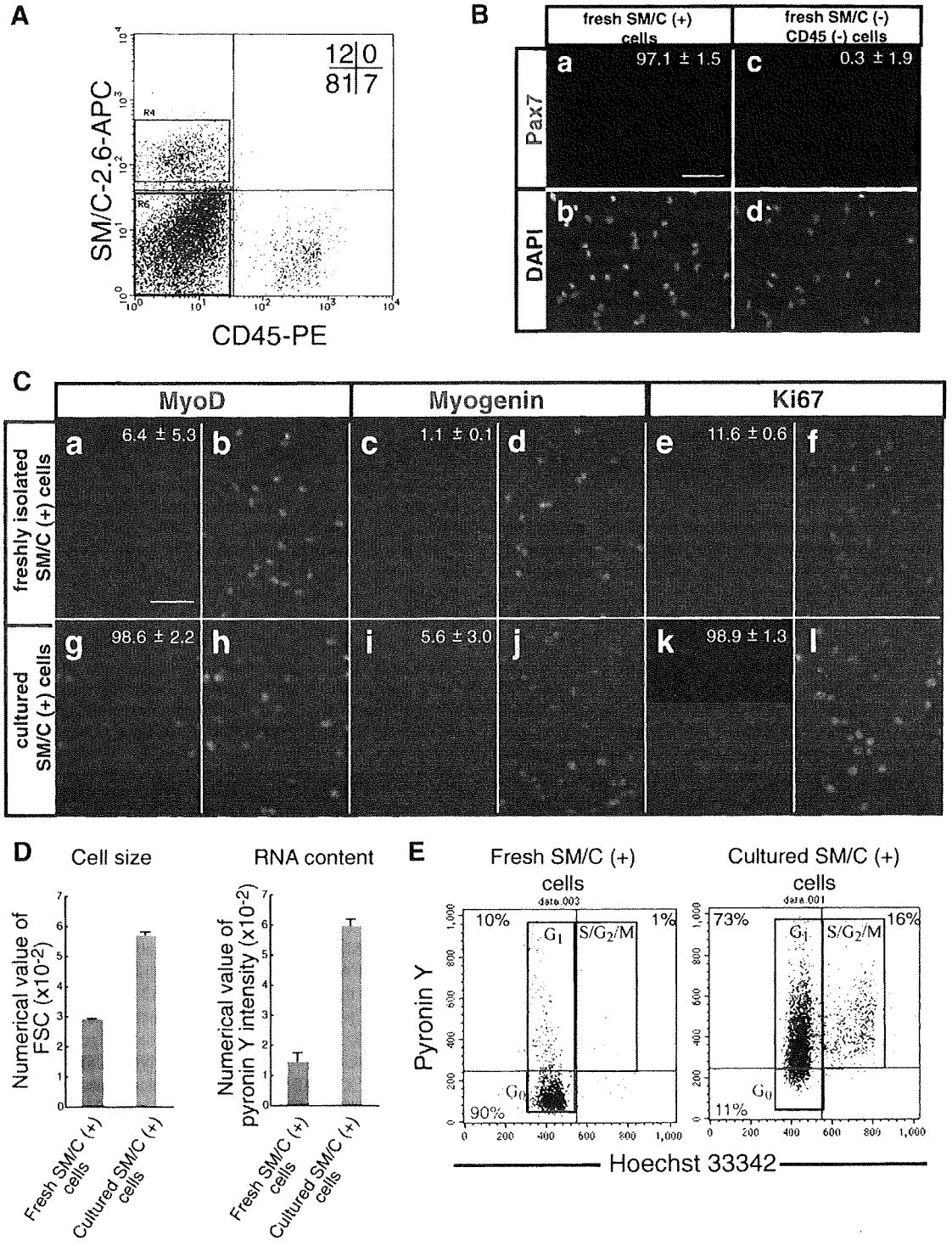

Figure 1. SM/C-2.6$^+$ cells isolated from skeletal muscle by fluorescence-activated cell sorting (FACS) are highly purified quiescent satellite cells and proliferate and express MyoD in culture. **(A):** Mononucleated cells prepared from uninjured limb muscles of adult mice were stained with anti-CD45 antibody and SM/C-2.6 monoclonal antibody. The SM/C-2.6$^+$ fraction (red square) and the SM/C-2.6$^-$/CD45$^-$ fraction (blue square) were collected for further analysis. **(B):** Freshly isolated SM/C-2.6$^+$ and SM/C-2.6$^-$/CD45$^-$ cells were stained with anti-Pax7 **(Ba, Bc)** antibody and DAPI **(Bb, Bd)**. The percentages of Pax7-positive cells in each cell fraction are shown. Cell fractionation was performed three times, and more than 300 cells from each fraction were counted. Scale bar: 50 μm. **(C):** Freshly isolated SM/C-2.6$^+$ cells and SM/C-2.6$^+$ cells cultured for 4 days in the presence of basic fibroblast growth factor were stained with antibodies to MyoD **(Ca, Cg)**, myogenin **(Cc, Ci)**, or Ki67 **(Ce, Ck)**. Percentages of MyoD-, myogenin-, or Ki67-positive cells are shown. Cell fractionation was performed three times, and more than 180 cells were counted each time. Nuclei were stained with DAPI **(Cb, Cd, Cf, Ch, Cj, Cl)**. Scale bar: 50 μm. **(D):** The mean value of FSC (cell size) and Pyronin Y intensity (RNA content) of freshly isolated SM/C-2.6$^+$ cells and satellite cells cultured in vitro. The value is an average of two independent experiments. **(E):** The percentages of cells in the G0 phase of the cell cycle were estimated by staining with Pyronin Y and Hoechst 33342. The number in the lower left of each FACS profile indicates the percentage of the G0 cells: 90% for fresh SM/C-2.6$^+$ cells and 11% for cultured SM/C-2.6$^+$ cells. Abbreviations: APC, allophycocyanin; DAPI, 4,6-diamidino-2-phenylindole; FSC, forward scatter; M, mitosis phase; PE, phycoerythrin; S, synthesis phase.

to be G0 cells [24]. Pyronin Y and Hoechst double staining shows that approximately 90% of fresh SM/C-2.6$^+$ cells were in the G0 phase of the cell cycle. In contrast, 90% of cultured SM/C-2.6$^+$ cells were cycling (Fig. 1E).

Thus, our procedure, which takes 5–6 hours in total to isolate 1–2 × 10^5 SM/C-2.6$^+$ cells from one C57BL/6 mouse, enables us to isolate satellite cells still in a quiescent and undifferentiated state. The yield corresponds to 10%–15% of the total mononucleated cells obtained from mouse hind limb muscles by enzymatic digestion. Therefore, in this report, we call freshly isolated SM/C-2.6$^+$ cells "quiescent satellite cells" and cultured, proliferating SM/C-2.6$^+$ cells "activated satellite cells." Our procedure was also applicable to dystrophin-deficient *mdx* muscle with modifications, although 30%–40% of *mdx* satellite cells are Ki67-positive (M. Ikemoto et al., submitted manuscript). Unfortunately, SM/C-2.6 did not react with satellite cells from dystrophin-deficient dystrophic dogs (data not shown).

Single Gene Analysis of Quiescent and Activated/Proliferating Satellite Cells

We prepared RNA samples from quiescent satellite cells and activated satellite cells and performed microarray analysis using Affymetrix GeneChips. Hybridization and data collection were performed four times using independent preparations of cells and RNA samples for each cell fraction. Raw data are available at http://www.ncbi.nlm.nih.gov/geo. The Gene Expression Omnibus accession number is GSE3483.

First, we compared the expression levels of individual genes in quiescent and activated states using GeneSpring software. We found that 507 genes (665 probes) were expressed in quiescent satellite cells at more than fivefold higher levels than in activated satellite cells (Fig. 2A). We roughly categorized these 507 genes into 11 gene groups: cell adhesion (15 genes), cell cycle regulation (26), proteolysis (21), cytoskeleton (13), cell surface (41), extracellular (61), immunoresponse (22), signal transduction (81), transcription (67), transport and metabolism (82), and unknown (78) based on Gene Ontology and listed all of them in supplemental online Table 1. On the other hand, 659 genes (814 probes) were upregulated (>fivefold) in the activated state (supplemental online Table 2). We also examined the gene expression of proliferating satellite cells/myoblasts in vivo that were directly isolated from regenerating muscle 2 days after cardiotoxin injection. The activated and proliferating satellite cells in vivo showed an expression profile quite similar to satellite cells cultured in vitro (data not shown).

Upregulation of Cell Cycle Regulators in Quiescent Satellite Cells

Under normal conditions, most satellite cells are in the G0 phase of the cell cycle, possibly preventing their premature exhaustion. It is of note that nine genes encoding negative regulators of the cell cycle were highly upregulated in the quiescent stage: *Rgs2* (*regulator of G-protein signaling 2*) (×69, ×23), *Rgs5* (×37, ×21), *Pmp22* (*peripheral myelin protein 22*)/*Gas3* (growth arrest specific 3) (×25), *Cdkn1c* (cyclin-dependent kinase inhibitor 1C)/*p57* (×14), *Spry1* (sprouty homolog 1) (×11), *Gas1* (×7, ×6), *Reck* (reversion-inducing-cysteine-rich protein with kazal motifs) (×6), *Ddit3* (DNA-damage inducible transcript 3) (×6), and *Trp63* (transformation-related protein 63) (×5) (supplemental online Table 1). Reverse transcription (RT)-PCR confirmed that *Rgs2*, *Pmp22*, *p57*, and *Spry1* are highly expressed in quiescent satellite cells and downregulated in activated satellite cells (Fig. 2Ba).

Cyclin-dependent kinase inhibitors (CKIs) play a key role in controlling the cell cycle in many cell types. p21 (CIP1) triggers the cell cycle exit of proliferating myoblasts to initiate myoblast terminal differentiation in response to differentiation signals [25]. p57 (KIP2) is induced in myoblasts upon differentiation. Gene targeting experiments showed that these two CKIs redundantly control cell cycle exit during myogenesis [26]. Compared with irreversible cell cycle arrest upon differentiation, however, attainment of a reversible G0 state by satellite cells is poorly understood. In vitro studies suggested that Rb family members p130 and p27 are involved in the reversible cell cycle exit of proliferating myoblasts to return satellite cells to quiescence [16]. In our experiments, p21 (×0.5), p27 (×1.5), and p130 (×2–3) were not significantly upregulated in quiescent satellite cells. Reflecting the levels of p57 mRNA, p57 protein was found in more than 90% of freshly isolated SM/C-2.6$^+$ cells (Fig. 2Ca). Whether p57 is required for acquisition and maintenance of quiescence of satellite cells remains to be determined in a future study.

Upregulation of Myogenic Inhibitors in Quiescent Satellite Cells

Quiescent satellite cells barely express myogenic basic helix-loop-helix (bHLH) factors. Activity of the *Myf-5* locus was revealed through a reporter gene, but Myf-5 protein is hardly detected in dormant satellite cells. On activation, satellite cells upregulate Myf5 and start to express MyoD [27] (Fig. 1). Our microarray analyses revealed that several myogenic inhibitory molecules were upregulated in quiescent satellite cells: *Bmp6* (*bone morphogenetic protein 6*) (×214), *Bmp4* (×66), *Bmp2* (×82), *Heyl* (*hairy/enhancer-of-split related with YRPW motif-like*)/*Herp3*/*Hrt3*/*hesr3* (×101, ×33, ×32), *Musculin*/*MyoR* (×83), *Notch3* (×9). Upregulation of *Bmp4*, *Bmp6*, *Msc*/*MyoR*, and *Heyl* in quiescent satellite cells was confirmed by RT-PCR (Fig. 2Bb). BMP4 is reported to negatively regulate MyoD expression in somite myogenesis [28] and differentiation of satellite cells, where BMP4-induced inhibition of myogenic differentiation requires Notch signaling [29]. Notch signaling is reported to inhibit the differentiation of myoblasts by repression of MyoD expression [30]. In postnatal muscle, Notch signaling controls satellite cell activation and their cell fate [31], and insufficient upregulation of the Notch ligand Delta is casually related to impaired regeneration of aged muscle [32]. Among several molecules in the Notch signaling pathway, our microarray analysis showed that *Notch3* and one of the Notch-effector genes, *Heyl*, are highly expressed in quiescent satellite cells. When cross-sections of normal mouse tibialis anterior (TA) muscle were stained with specific antibodies, HeyL was found in nearly all Pax7-positive nuclei, and Notch3 was expressed on the surface of mononuclear cells beneath the basal lamina (Fig. 2Cb, 2Cc). These results suggest that Notch3 and HeyL play roles in Notch signaling to inhibit muscle differentiation of satellite cells. Musculin/MyoR is a bHLH transcription factor originally cloned as a repressor of MyoD [33]. Musculin-null mice do not exhibit any skeletal muscle defect, but musculin is likely to negatively regulate MyoD in muscle regeneration [34].

In addition to negative regulators, two positive regulators of myogenesis, *Gli2* (*GLI-Kruppel family member GLI2*) (×29, ×13) and *Meox2* (*mesenchyme homeobox 2*) (×17), are preferentially expressed in quiescent satellite cells. Gli2 directly upregulates Myf5 [35], and Meox1 and 2 regulate Pax3 and Pax7 expressions [36]. These observations suggest that Gli2 and Meox2 maintain lineage identity in quiescent satellite cells.

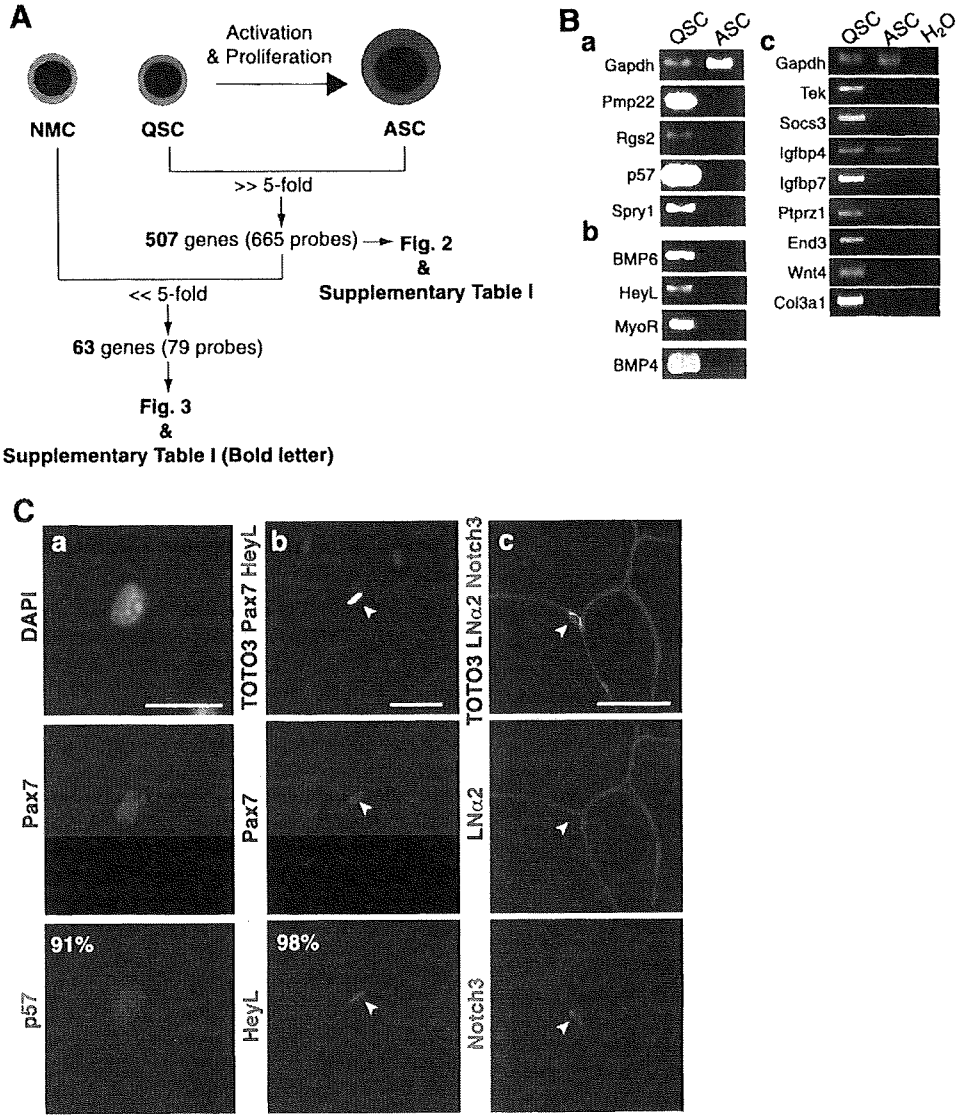

Figure 2. Identification of the genes expressed at higher levels in QSC than in ASC. **(A):** Outline of gene expression analysis at single gene level. Sixty-three genes out of 507 genes were found to be expressed at a higher level (more than fivefold) in quiescent satellite cells than in NMC. We applied Student's *t* test (p value .05) with multiple testing corrections (Benjamini and Hochberg false discovery rate). **(B):** Reverse transcription-polymerase chain reaction of eight relevant genes involved in cell cycle regulation **(Ba)**, inhibition of myogenesis **(Bb)**, or other biological process **(Bc)** (Table 1). Total RNAs were isolated from fluorescence-activated cell sorting-sorted SM/C-2.6$^+$ cells (QSC) and cultured SM/C-2.6$^+$ cells (ASC). *Gapdh* is control. **(Ca):** Mononucleated cells from intact skeletal muscle were stained with anti-p57 (red), Pax7 (green), and DAPI (blue) immediately after sorting. **(Cb, Cc):** Cross-sections of normal skeletal muscle were stained with antibodies to HeyL (red in **[Cb]**), Notch3 (red in **[Cc]**), Pax7 (green in **[Cb]**), or laminin α2 chain (green in **[Cc]**). More than 90% of Pax7-positive cells were positive for p57. Nearly all Pax7-positive cells expressed HeyL. Notch3 was expressed on the cell surface on satellite cells. Nuclei were stained with TOTO3 (blue). Scale bar: 20 μm. Abbreviations: ASC, activated satellite cells; DAPI, 4,6-diamidino-2-phenylindole; LNα2, laminin α2; NMC, nonmyogenic cells; QSC, quiescent satellite cells.

Identification of Quiescent Satellite Cell-Specific Genes

To identify quiescent satellite cell-specific genes from 507 genes (Fig. 2A), we next prepared RNA samples from nonmyogenic cells (SM/C-2.6$^-$/CD45$^-$ in Fig. 1A) and performed microarray analysis using Affymetrix GeneChips. Statistical analysis validated that 63 genes out of 507 genes were preferentially expressed (>fivefold) in quiescent satellite cells compared with nonmyogenic cells or activated satellite cells (genes in bold letters in supplemental online Table 1).

To confirm the microarray results, we next performed RT-PCR on 14 genes of interest. In addition to microarray samples, the results for TA muscle and a myogenic cell line, C2C12 cells, are also shown (Fig. 3). Two well-established satellite cell markers (Pax7 and M-cadherin) were expressed not only in quiescent satellite cells but also in activated satellite cells and/or C2C12 cells. In contrast, two cell surface molecules, Odz4, a mouse homolog of the *Drosophila* pair-rule gene *Odd Oz* [37], and CTR, a signaling molecule Tribbles1, and two extracellular molecules, endothelin3 and chordin-like2, were all confirmed to be expressed exclusively in quiescent satellite cells.

Gene Set Enrichment Analysis Revealed Gene Groups Upregulated in Quiescent Satellite Cells

Single-gene analysis permitted us to identify candidate genes that regulate quiescence and undifferentiated state of satellite cells in vivo. To complement the analysis at the single gene

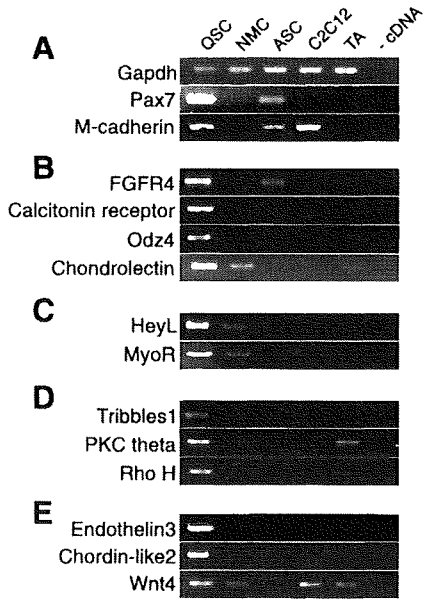

Figure 3. Reverse transcription-polymerase chain reaction (RT-PCR) of quiescent satellite cell-specific genes. Expression levels of quiescent satellite cell-specific genes in fluorescence-activated cell sorting-sorted SM/C-2.6$^+$ cells (lane 1), SM/C-2.6$^-$/CD45$^-$ nonmyogenic cells (lane 2), cultured SM/C-2.6$^+$ cells (lane 3), C2C12 cells (lane 4), and TA muscle (lane 5) were confirmed by RT-PCR. The genes are categorized into five groups: well-known satellite cell markers (**A**), cell surface receptors (**B**), transcription factors (**C**), signal molecules (**D**), and extracellular molecules (**E**). Lane 6 is the reaction without cDNA templates. Abbreviations: ASC, activated satellite cells; NMC, nonmyogenic cells; QSC, quiescent satellite cells; TA, tibialis anterior.

level, we performed gene set enrichment analysis [22]. GSEA is an analytical method that identifies small but coordinated changes of predefined gene sets but not up- or downregulation of individual genes, which therefore would help us to identify important signaling pathways or regulatory mechanisms for satellite cells. We used GO annotations [23] to group all genes on GeneChips and tried to extract gene sets that are upregulated as a whole in quiescent satellite cells compared with activated and proliferating satellite cells (Fig. 4). When all genes were categorized into 1,674 gene sets according to their biological process ontology, only three gene sets were judged to be coordinately upregulated in quiescent satellite cells (FDR < 0.25): cell-cell adhesion, regulation of cell growth, and transmembrane receptor protein tyrosine phosphatase signaling pathway (Table 1). When all genes were grouped into 1,698 gene sets according to cellular component ontology, three gene sets, insoluble fraction, extracellular region, and collagens, were found to be coordinately upregulated in quiescent satellite cells compared with activated/proliferating satellite cells (Table 1). When grouped into 412 gene sets based on their predicted molecular functions, three gene sets, extracellular matrix structural constituent conferring tensile strength, copper ion binding, and lipid transporter activity, were found to be coordinately upregulated in quiescent satellite cells (Table 1). Seven genes listed in Table 1 (*Tek, Socs3, Igfbp7, Ptprz1, End3, Wnt4,* and *Col3a1*) were confirmed to be upregulated in quiescent satellite cells by RT-PCR (Fig. 2Bc). A more detailed discussion on GSEA results is in the supplemental online Discussion.

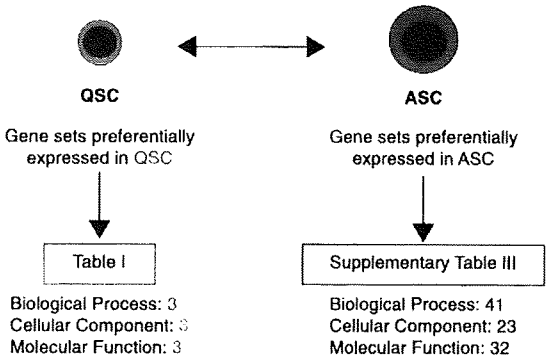

Figure 4. Gene set enrichment analysis (GSEA) of quiescent and activated satellite cells. Summary of GSEA comparing QSC with ASC using gene sets based on three major Gene Ontology trees: cellular component, biological process, and molecular function. Gene sets with high enrichment score (1 − [false discovery rate q value] are >0.75) are listed in Table 1 and supplemental online Table 3. Abbreviations: ASC, activated satellite cells; QSC, quiescent satellite cells.

Gene Sets That Are Coordinately Upregulated upon Activation

Many gene sets were found to be coordinately upregulated in activated/proliferating satellite cells compared with quiescent satellite cells (Fig. 4). These are involved in active synthesis of DNA, RNA and protein, progression of cell cycle (*Cdc2a, Cdc20, Cdc25c, Ccnb1, Ccna2,* etc.), mitochondrial activities, and so on. The gene sets are all listed in supplemental online Table 3. The results well reflect active cell cycling and high metabolic activity of satellite cells.

Expression of Cell-Cell Adhesion Molecules on Satellite Cells

Both single gene analysis and GSEA suggest that cell-cell adhesion is one of the key elements in the regulation of satellite cells. Preferential expression of the following genes in quiescent satellite cells was confirmed by RT-PCR and quantitative PCR (supplemental online Fig. 1A, 1B): *VE-cadherin* (*cadherin 5*), *Vcam1*, *Icam1*, *Cldn5* (*claudin 5*), *Esam* (*endothelial cell-specific adhesion molecule*), and *Pcdhb9* (*protocadherin beta 9*). To date, several cell surface markers for satellite cells have been identified, including M-cadherin, syndecan3, syndecan4, c-met, Vcam-1, NCAM-1, and CD34 [5, 38–43]. Vascular endothelial (VE)-cadherin, Icam1, claudin5, Esam, and Pcdhb9 should be added to the list. Because *Esam* is upregulated in long-term hematopoietic stem cells and mammary gland side population cells [44, 45], the expression of *Esam* in quiescent satellite cells is quite intriguing. When transverse sections of adult skeletal muscle were stained with specific antibodies, M-cadherin was found at the site of contact between satellite cells and myofibers (supplemental online Fig. 1C) [38]. Vcam-1 and VE-cadherin proteins are also detected at the boundary of satellite cells and myofibers. Although their roles in regulation of satellite cells remain to be determined, our observations suggest that cell-cell adhesion molecules have critical roles in keeping satellite cells in an undifferentiated and quiescent state and in protecting satellite cells from cell death. We also confirmed that FACS with Vcam-1 anti-

Table 1. Gene sets upregulated in quiescent satellite cells and genes with high enrichment scores

	1 − (FDR q value)
Biological process	
Cell-cell adhesion	.791
Tek, Vcam1, Icam2, Cldn5, Cdh5, Icam1	
Regulation of cell growth	.787
Socs3, Htra1, Htra3, Ctgf, Igfbp4, Creg1, Igfbp7, Epc1, Cyr61, Crim1, Nov, Igfbp6, Nedd9	
Transmembrane receptor protein tyrosine phosphatase signaling pathway	.751
Ptprz1, Ptprf, Ptprb, Ptprd, Ptprk, Ptprs, Ptprr	
Cellular component	
Insoluble fraction	.786
Dmd, Dag1, Plec1, Des, Hspb1	
Extracellular region	.766
Sepp1, Htra1, Edn3, Cxcl1, Loxl1, Htra3, Thbs4, Ctgf, Ntf3, Twsg1, Ccl27, Rarres2, Ltbp3, Igfbp4, Apoe, Igf1, Ibsp, Trf, Pthlh, Polydom, Ccl11, Abca3, Thbs3, Wnt4, Prss1, Vwa1, Comp, Nppc, Cyp4v3, Ccl19, Nts, Fbln2, Cocoacrisp, Cxcl2, Igfbp7, C1r, Thbs2, Ccl6, Calca, Cyr61, Icosl, Ccl21c, Crim1, Il6, Degb10, Cxcl9, Csng, C3, Cxcl10, Cxcl14, Inhbb, Il15, Nov, Igfbp6, Mglap, Dkk2, Tnfsf12, Ifnb1, Tfpi2, Cxcl11, Il18, Pi16, Pycard, Lzp-s, Stc1, Lyzs	
Collagen	.766
Col3a1, Col6a2, Col17a1, Col1a2, Col15a1, Col6a3, Col5a3, Col1a1, Col4a1, Col5a1, Col11a1	
Molecular function	
Extracellular matrix structural constituents conferring tensile strength	.774
Col3a1, Col6a2, Col17a1, Col1a2, Col15a1, Col6a3, Col16a1, Col1a1, Col4a1, Col4a5, Col5a1, Col11a1, Col11a2, Col9a1, Col4a2, Col4a4	
Copper ion binding	.764
Aoc3, Cp, Loxl1, Mt1, Atp7a, Heph, Loxl2, Nr1h3	
Lipid transporter activity	.752
Vldlr, Lpl, Apoe, Sorl1, Ldlr, Gpld1, Lrp1	

Gene names are listed according to the rank of enrichment scores. Underlined genes (46/118 genes) are also listed in supplemental online Table 1.
Abbreviation: FDR, false discovery rate.

body efficiently enriches quiescent satellite cells as SM/C-2.6 does (supplemental online Fig. 2).

Calcitonin Receptor Is Sharply Downregulated on Activated Satellite Cells and Reappeared on Renewed Satellite Cells During Muscle Regeneration

RT-PCR verified that CTR is exclusively expressed in quiescent satellite cells but not in activated satellite cells or in nonmyogenic cells (Fig. 3). In addition, we confirmed that calcitonin mRNA is expressed in satellite cells (data not shown). Therefore, we examined the expression of CTR protein in vivo using immunohistochemistry. As shown in Figure 5A, CTR protein was observed in Pax7-positive mononuclear cells beneath the basal lamina in uninjured muscle. We next stained cross-sections of regenerating muscle with anti-CTR antibody. Three days after cardiotoxin injection, many activated satellite cells were stained with anti-M-cadherin antibodies, but CTR expression was not detected on activated satellite cells on the serial sections (Fig. 5B). Furthermore, there were no $Pax7^+/CTR^+$ cells on muscle sections until 7 days after injury (cardiotoxin [CTX]-7d), when $Pax7^+/CTR^+$ cells were again found at the periphery of centrally nucleated, relatively large myofibers but not of small regenerating fibers (Fig. 5C, 5D). The number of $Pax7^+/CTR^+$ cells gradually increased thereafter and reached the level of uninjured muscle by CTX-14d (Fig. 5D). Interestingly, approximately 20% of $Pax7^+/CTR^+$ cells on CTX-7d were found outside the basal lamina (Fig. 5E). This atypical position of satellite cells was transient, and the ratio of satellite cells residing beneath the basal lamina increased during myofiber maturation (data not shown). Taken together, the results suggest that the expression of CTR is found not only on quiescent satellite cells but also on newly formed satellite cells that are closely associated with maturing myofibers.

Calcitonin Inhibits Activation of Quiescent Satellite Cells

To investigate the roles of CTR in the regulation of satellite cells, eel calcitonin, elcatonin, was added to the culture of quiescent satellite cells in vitro before or after activation. Addition of calcitonin before activation significantly inhibited BrdU uptake by quiescent satellite cells (Fig. 6A) but not by already activated satellite cells (Fig. 6A). Interestingly, a short exposure (0.5 hours) to calcitonin was enough to suppress the activation of quiescent satellite cells (Fig. 6B).

MyoD staining of satellite cells revealed that calcitonin/CTR signaling delays the induction of MyoD in quiescent satellite cells (Fig. 6C). The lower percentage of Ki67-positive cells in calcitonin-treated satellite cells also indicated that calcitonin delays the entry of quiescent satellite cells into the cell cycle (Fig. 6C). Calcitonin-treated cells were considerably smaller than control cells on the second day of culture (Fig. 6D), again indicating delayed activation of satellite cells in the presence of calcitonin. A terminal deoxynucleotidyl transferase dUTP nick-end labeling assay excludes the possibility that calcitonin induced apoptosis in satellite cells (Fig. 6E).

To further investigate the effects of calcitonin on activation of quiescent satellite cells, we prepared living single muscle fibers from mouse extensor digitorum longus muscles by using the collagenase digestion method [20] and plated them onto Matrigel-coated 24-well plates at a density of one fiber per well in the presence or absence of calcitonin. In control wells, many satellite cells had detached and migrated from the myofibers 2 days after plating (Fig. 6F). Calcitonin significantly reduced the numbers of satellite cells that had detached from myofibers (Fig. 6F). It was reported that

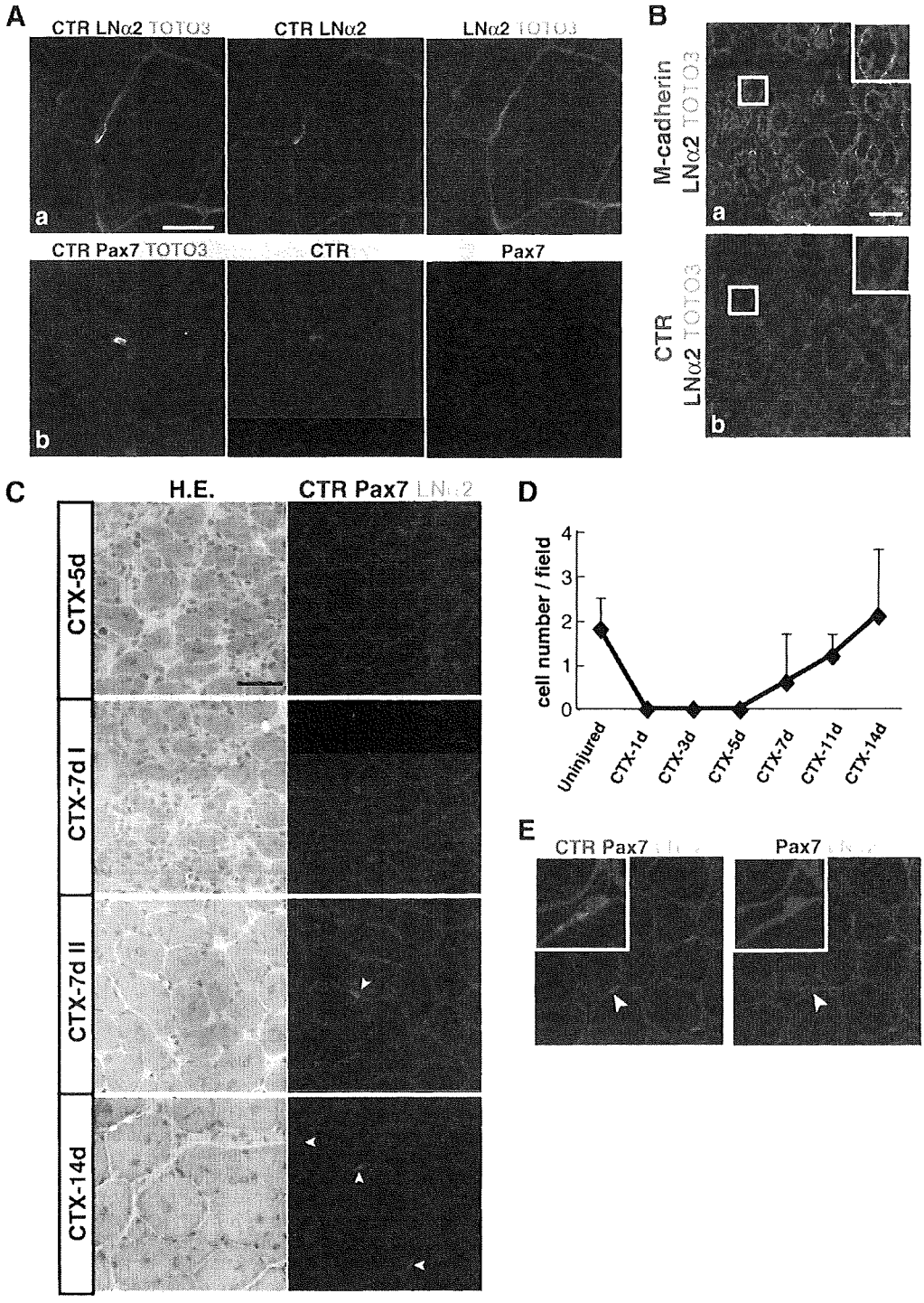

Figure 5. Reappearance of CTR- and Pax7-positive satellite cells in regenerating muscle 7 days after cardiotoxin injection. **(A):** Cross-sections of uninjured skeletal muscle were stained with antibodies to calcitonin receptor (red), laminin $\alpha 2$ chain (green in [Aa]), or Pax7 (green in [Ab]). Nuclei were stained with TOTO3 (blue). Scale bar: 20 μm. **(B):** Three days after CTX injection, regenerating muscles were dissected, and serial cross-sections were stained with antibodies to M-cadherin (red in **[Ba]**) or CTR (red in **[Bb]**) and anti-laminin $\alpha 2$ (green in **[Ba, Bb]**) antibodies. Insets show close-ups of marked areas by white squares. Nuclei were stained with TOTO3 (blue). Scale bar: 40 μm. **(C):** Tibialis anterior muscles were sampled at five (CTX-5d), seven (CTX-7d), and 14 days (CTX-14d) after CTX injection. Sections were coimmunostained with anti-CTR (red), Pax7 (green), and laminin $\alpha 2$ chain (blue) antibodies. Serial sections were stained with H.E. Note that $Pax7^+/CTR^+$ cells were first detected on the seventh day of regeneration around regenerating muscle fibers with a large diameter (CTX-7d II) but not around small-sized fibers (CTX-7d I). Arrowheads indicate CTR-positive Pax7-positive cells. Scale bar: 40 μm. **(D):** Numbers of $Pax7^+/CTR^+$ cells per field at 1, 3, 5, 7, 11, and 14 days after CTX injection. $Pax7^+/CTR^+$ cells were counted in 12–21 randomly selected fields in the regenerating area. The average is shown with SD. **(E):** Cross-sections of regenerating muscle 7 days after CTX injection were coimmunostained with CTR (red), Pax7 (green), and laminin $\alpha 2$ (blue). A typical $Pax7^+/CTR^+$ satellite cell outside the basal lamina is shown (arrowheads). Scale bar: 20 μm. Abbreviations: CTR, calcitonin receptor; CTX, cardiotoxin; d, day; H.E., hematoxylin and eosin; LN$\alpha 2$, laminin $\alpha 2$.

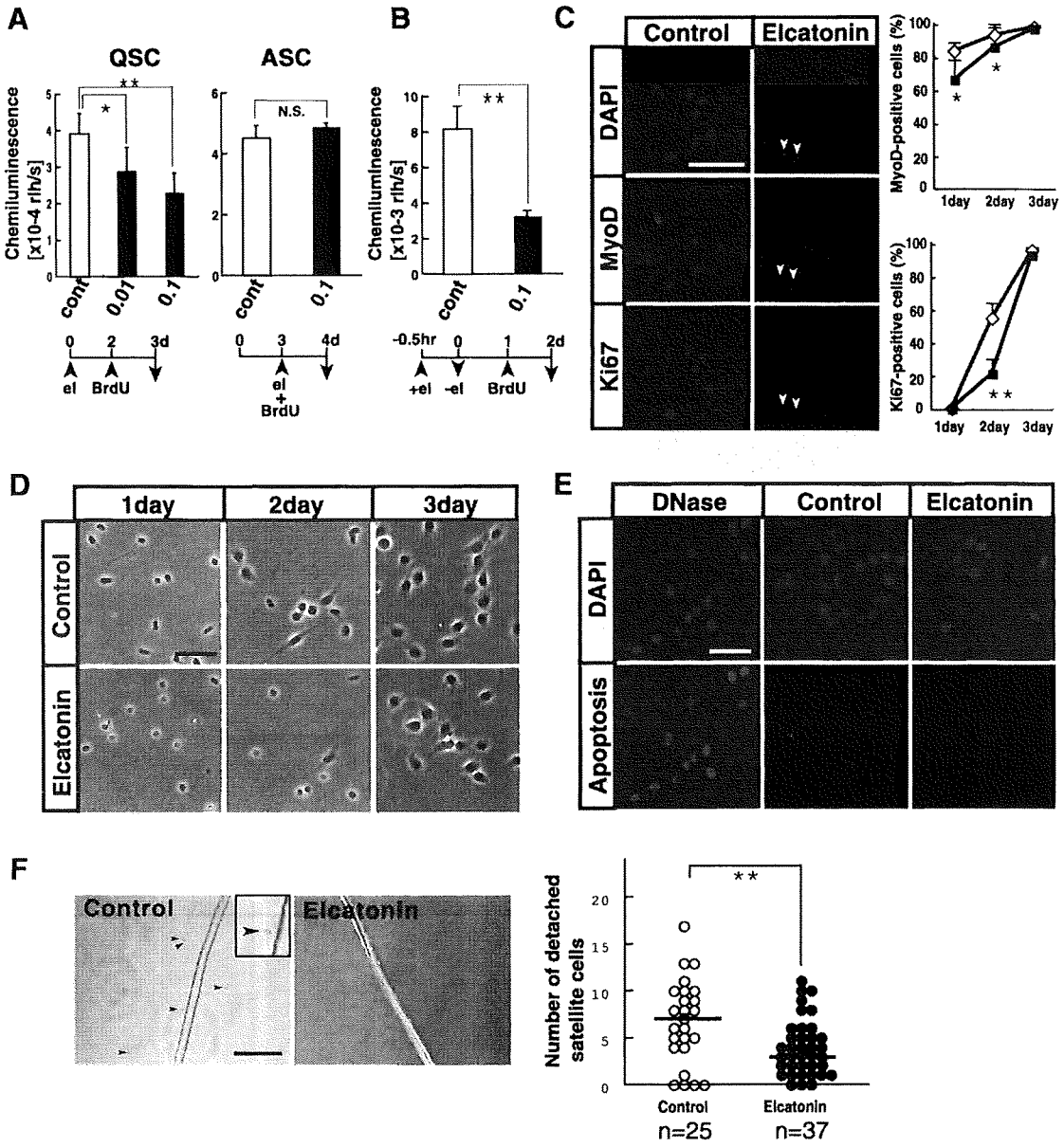

Figure 6. Calcitonin receptor agonist, elcatonin, suppresses activation of quiescent satellite cells. **(A):** Freshly isolated SM/C-2.6$^+$ cells (QSC) and cultured SM/C-2.6$^+$ cells (ASC) were grown in the presence (black) or absence (white) of eel calcitonin, elcatonin. Left: QSC were cultured for 2 days with (0.01 U/ml or 0.1 U/ml) or without elcatonin and then cultured for an additional 24 hours in the presence of BrdU. Right: QSC were cultured for 3 days and then cultured for 24 hours in the presence or absence of elcatonin and BrdU. The vertical axis shows the mean BrdU uptake by satellite cells of three experiments with SD; * $p < .05$, ** $p < .01$ (analysis of variance [ANOVA] test). **(B):** BrdU uptake by QSC exposed to elcatonin for 30 minutes prior to plating. Values are means with SD ($n = 3$); ** $p < .01$. **(C):** QSC cultured in the presence or absence of 0.1 U/ml elcatonin for 2 days were stained with anti-MyoD (red) or Ki67 (green) antibodies. Nuclei were stained with DAPI (blue). Arrowheads indicate MyoD- and Ki67-negative satellite cells. Graphs show the frequency of MyoD- or Ki67-positive cells 1, 2, or 3 days after plating with (closed square) or without (open diamond) elcatonin. More than 100 cells were counted. Values are means with SD; * $p < .05$, ** $p < .01$. Scale bar: 50 μm. **(D):** Phase contrast images of satellite cells 1, 2, and 3 days after plating in the presence or absence of 0.1 U/ml elcatonin. Note that many elcatonin-treated satellite cells are smaller than nontreated cells 2 days after plating. Scale bar: 50 μm. **(E):** Terminal deoxynucleotidyl transferase dUTP nick-end labeling assay on satellite cells cultured with or without elcatonin for 2 days. Apoptotic cells are in red. Nuclei were stained with DAPI (blue). As a positive control, satellite cells were pretreated with DNase. Scale bar: 50 μm. **(F):** Activation of satellite cells on myofibers in vitro. Isolated muscle fibers were plated at a density of one fiber per well and cultured with or without elcatonin (0.1 U/ml) for 2 days, and the numbers of satellite cells that had detached and migrated from each muscle fiber (arrowheads) were counted. Inset is a close-up image of a detached satellite cell. Scale bar: 100 μm. ANOVA t test, ** $p < .01$. Abbreviations: ASC, activated satellite cells; BrdU, 5-bromo-2′-deoxyuridine; d, days; DAPI, 4,6-diamidino-2-phenylindole; el, elcatonin; hr, hours; NS, nonsignificant; QSC, quiescent satellite cells.

calcitonin signaling was mediated via cAMP [46]. An analog of cAMP, dibutyryl cAMP, and an activator of adenylate cyclase, forskolin, also attenuated the activation of satellite cells in vitro (data not shown). Collectively, our results suggest that calcitonin/CTR signaling inhibits activation of satellite cells but not their proliferation or survival. The downstream target molecules of calcitonin/CTR remain to be determined.

CONCLUSION

Single gene-level analysis revealed several candidate genes that negatively regulate cell cycling of satellite cells. Furthermore, our results suggested that satellite cells express both myogenic and antimyogenic molecules to maintain their delicate state.

GSEA showed that dormant satellite cells coordinately express gene groups involved in cell-cell adhesion, cell-extracellular matrix interaction, copper and iron homeostasis, lipid transport, and regulation of cell growth. Although the result shows one aspect of regulation of quiescent satellite cells, more elaborate gene grouping might be needed to further understand the molecular regulation of quiescent satellite cells.

Finally, we showed that calcitonin receptor is specifically expressed on quiescent satellite cells and transmits signals that attenuate the entry of quiescent satellite cells into the cell cycle. Our results would greatly facilitate the investigation of molecular regulation of satellite cells in both physiological and pathological conditions.

ACKNOWLEDGMENTS

This work was supported by Grants for Research on Nervous and Mental Disorders (16B-2), Health Science Research Grants for Research on the Human Genome and Gene Therapy (H16-genome-003), for Research on Brain Science (H15-Brain-021) from the Japanese Ministry of Health, Labor and Welfare, Grants-in-Aids for Scientific Research (14657158, 153,90281, and 165,90333) from the Japanese Ministry of Education, Culture, Sports, Science and Technology, and "Ground-Based Research Program for Space Utilization" promoted by Japan Space Forum.

DISCLOSURE OF POTENTIAL CONFLICTS OF INTEREST

The authors indicate no potential conflicts of interest.

REFERENCES

1 Bischoff R. Analysis of muscle regeneration using single myofibers in culture. Med Sci Sports Exerc 1989;21(suppl 5):S164–S172.
2 Partridge T. Reenthronement of the muscle satellite cell. Cell 2004;119: 447–448.
3 Mauro A. Satellite cell of skeletal muscle fibers. J Biophys Biochem Cytol 1961;9:493–495.
4 Schultz E, Gibson MC, Champion T. Satellite cells are mitotically quiescent in mature mouse muscle: an EM and radioautographic study. J Exp Zool 1978;206:451–456.
5 Cornelison DD, Wold BJ. Single-cell analysis of regulatory gene expression in quiescent and activated mouse skeletal muscle satellite cells. Dev Biol 1997;191:270–283.
6 Bischoff R. Satellite and stem cells in muscle regeneration. In: Engel AG, Franzini-Armstrong C, eds. Myology. Vol 1. New York: McGraw-Hill, 2004:66–86.
7 Collins CA, Olsen I, Zammit PS et al. Stem cell function, self-renewal, and behavioral heterogeneity of cells from the adult muscle satellite cell niche. Cell 2005;122:289–301.
8 Seale P, Sabourin LA, Girgis-Gabardo A et al. Pax7 is required for the specification of myogenic satellite cells. Cell 2000;102:777–786.
9 Grounds MD, Yablonka-Reuveni Z. Molecular and cell biology of skeletal muscle regeneration. Mol Cell Biol Hum Dis Ser 1993;3: 210–256.
10 Wagers AJ, Conboy IM. Cellular and molecular signatures of muscle regeneration: Current concepts and controversies in adult myogenesis. Cell 2005;122:659–667.
11 Asakura A, Komaki M, Rudnicki M. Muscle satellite cells are multipotential stem cells that exhibit myogenic, osteogenic, and adipogenic differentiation. Differentiation 2001;68:245–253.
12 Wada MR, Inagawa-Ogashiwa M, Shimizu S et al. Generation of different fates from multipotent muscle stem cells. Development 2002;129: 2987–2995.
13 Shefer G, Wleklinski-Lee M, Yablonka-Reuveni Z. Skeletal muscle satellite cells can spontaneously enter an alternative mesenchymal pathway. J Cell Sci 2004;117:5393–5404.
14 McCroskery S, Thomas M, Maxwell L et al. Myostatin negatively regulates satellite cell activation and self-renewal. J Cell Biol 2003;162: 1135–1147.
15 Thomas M, Langley B, Berry C et al. Myostatin, a negative regulator of muscle growth, functions by inhibiting myoblast proliferation. J Biol Chem 2000;275:40235–40243.
16 Cao Y, Zhao Z, Gruszczynska-Biegala J et al. Role of metalloprotease disintegrin ADAM12 in determination of quiescent reserve cells during myogenic differentiation in vitro. Mol Cell Biol 2003;23: 6725–6738.
17 Carnac G, Fajas L, L'Honore A et al. The retinoblastoma-like protein p130 is involved in the determination of reserve cells in differentiating myoblasts. Curr Biol 2000;10:543–546.
18 Fukada S, Higuchi S, Segawa M et al. Purification and cell-surface marker characterization of quiescent satellite cells from murine skeletal muscle by a novel monoclonal antibody. Exp Cell Res 2004;296: 245–255.
19 Uezumi A, Ojima K, Fukada S et al. Functional heterogeneity of side population cells in skeletal muscle. Biochem Biophys Res Commun 2006;341:864–873.
20 Rosenblatt JD, Lunt AI, Parry DJ et al. Culturing satellite cells from living single muscle fiber explants. In Vitro Cell Dev Biol Anim 1995; 31:773–779.
21 Ojima K, Uezumi A, Miyoshi H et al. Mac-1(low) early myeloid cells in the bone marrow-derived SP fraction migrate into injured skeletal muscle and participate in muscle regeneration. Biochem Biophys Res Commun 2004;321:1050–1061.
22 Mootha VK, Lindgren CM, Eriksson KF et al. PGC-1alpha-responsive genes involved in oxidative phosphorylation are coordinately downregulated in human diabetes. Nat Genet 2003;34:267–273.
23 Ashburner M, Ball CA, Blake JA et al. Gene ontology: Tool for the unification of biology. The Gene Ontology Consortium. Nat Genet 2000;25:25–29.
24 Holyoake T, Jiang X, Eaves C et al. Isolation of a highly quiescent subpopulation of primitive leukemic cells in chronic myeloid leukemia. Blood 1999;94:2056–2064.
25 Missero C, Calautti E, Eckner R et al. Involvement of the cell-cycle inhibitor Cip1/WAF1 and the E1A-associated p300 protein in terminal differentiation. Proc Natl Acad Sci U S A 1995;92:5451–5455.
26 Zhang P, Wong C, Liu D et al. p21(CIP1) and p57(KIP2) control muscle differentiation at the myogenin step. Genes Dev 1999;13:213–224.
27 Cooper RN, Tajbakhsh S, Mouly V et al. In vivo satellite cell activation via Myf5 and MyoD in regenerating mouse skeletal muscle. J Cell Sci 1999;112:2895–2901.
28 Reshef R, Maroto M, Lassar AB. Regulation of dorsal somitic cell fates: BMPs and Noggin control the timing and pattern of myogenic regulator expression. Genes Dev 1998;12:290–303.
29 Dahlqvist C, Blokzijl A, Chapman G et al. Functional Notch signaling is required for BMP4-induced inhibition of myogenic differentiation. Development 2003;130:6089–6099.
30 Kuroda K, Tani S, Tamura K et al. Delta-induced Notch signaling mediated by RBP-J inhibits MyoD expression and myogenesis. J Biol Chem 1999;274:7238–7244.
31 Conboy IM, Rando TA. The regulation of Notch signaling controls satellite cell activation and cell fate determination in postnatal myogenesis. Dev Cell 2002;3:397–409.
32 Conboy IM, Conboy MJ, Smythe GM et al. Notch-mediated restoration of regenerative potential to aged muscle. Science 2003;302: 1575–1577.
33 Lu J, Webb R, Richardson JA et al. MyoR: A muscle-restricted basic helix-loop-helix transcription factor that antagonizes the actions of MyoD. Proc Natl Acad Sci U S A 1999;96:552–557.
34 Zhao P, Hoffman EP. Musculin isoforms and repression of MyoD in muscle regeneration. Biochem Biophys Res Commun 2006;342: 835–842.
35 Gustafsson MK, Pan H, Pinney DF et al. Myf5 is a direct target of long-range Shh signaling and Gli regulation for muscle specification. Genes Dev 2002;16:114–126.
36 Mankoo BS, Skuntz S, Harrigan I et al. The concerted action of Meox homeobox genes is required upstream of genetic pathways essential for the formation, patterning and differentiation of somites. Development 2003;130:4655–4664.

37 Zhou XH, Brandau O, Feng K et al. The murine Ten-m/Odz genes show distinct but overlapping expression patterns during development and in adult brain. Gene Expr Patterns 2003;3:397–405.
38 Irintchev A, Zeschnigk M, Starzinski-Powitz A et al. Expression pattern of M-cadherin in normal, denervated, and regenerating mouse muscles. Dev Dyn 1994;199:326–337.
39 Cornelison DD, Filla MS, Stanley HM et al. Syndecan-3 and syndecan-4 specifically mark skeletal muscle satellite cells and are implicated in satellite cell maintenance and muscle regeneration. Dev Biol 2001;239: 79–94.
40 Beauchamp JR, Heslop L, Yu DS et al. Expression of CD34 and Myf5 defines the majority of quiescent adult skeletal muscle satellite cells. J Cell Biol 2000;151:1221–1234.
41 Jesse TL, LaChance R, Iademarco MF et al. Interferon regulatory factor-2 is a transcriptional activator in muscle where It regulates expression of vascular cell adhesion molecule-1. J Cell Biol 1998; 140:1265–1276.
42 Illa I, Leon-Monzon M, Dalakas MC. Regenerating and denervated human muscle fibers and satellite cells express neural cell adhesion molecule recognized by monoclonal antibodies to natural killer cells. Ann Neurol 1992;31:46–52.
43 Charge SB, Rudnicki MA. Cellular and molecular regulation of muscle regeneration. Physiol Rev 2004;84:209–238.
44 Forsberg EC, Prohaska SS, Katzman S et al. Differential expression of novel potential regulators in hematopoietic stem cells. PLoS Genet 2005;1:e28.
45 Behbod F, Xian W, Shaw CA et al. Transcriptional profiling of mammary gland side population cells. STEM CELLS 2006;24:1065–1074.
46 Becker K, Muller B, Nylen E et al. Calcitonin Gene Family of Peptides. Vol 1. 2nd ed. New York: Academic Press, 2002.


See www.StemCells.com for supplemental material available online.

Gene Therapy (2007) 14, 1249–1260

www.nature.com/gt

ORIGINAL ARTICLE

Injection of a recombinant AAV serotype 2 into canine skeletal muscles evokes strong immune responses against transgene products

K Yuasa[1,2], M Yoshimura[1], N Urasawa[1], S Ohshima[1], JM Howell[3], A Nakamura[1], T Hijikata[2], Y Miyagoe-Suzuki[1] and S Takeda[1]

[1]*Department of Molecular Therapy, National Institute of Neuroscience, National Center of Neurology and Psychiatry, Kodaira, Tokyo, Japan;* [2]*Research Institute of Pharmaceutical Sciences, Faculty of Pharmacy, Musashino University, Nishi-tokyo, Tokyo, Japan and* [3]*Division of Veterinary and Biomedical Sciences, Murdoch University, Perth, Western Australia, Australia*

Using murine models, we have previously demonstrated that recombinant adeno-associated virus (rAAV)-mediated micro-dystrophin gene transfer is a promising approach to treatment of Duchenne muscular dystrophy (DMD). To examine further therapeutic effects and the safety issue of rAAV-mediated microdystrophin gene transfer using larger animal models, such as dystrophic dog models, we first investigated transduction efficiency of rAAV in wild-type canine muscle cells, and found that rAAV2 encoding β-galactosidase effectively transduces canine primary myotubes in vitro. *Subsequent rAAV2 transfer into skeletal muscles of normal dogs, however, resulted in low and transient expression of β-galactosidase together with intense cellular infiltrations* in vivo, *where cellular and humoral immune responses were remarkably activated. In contrast, rAAV2 expressing no transgene elicited no cellular infiltrations. Co-administration of immunosuppressants, cyclosporine and mycophenolate mofetil could partially improve rAAV2 transduction. Collectively, these results suggest that immune responses against the transgene product caused cellular infiltration and eliminated transduced myofibers in dogs. Furthermore,* in vitro *interferon-γ release assay showed that canine splenocytes respond to immunogens or mitogens more susceptibly than murine ones. Our results emphasize the importance to scrutinize the immune responses to AAV vectors in larger animal models before applying rAAV-mediated gene therapy to DMD patients.*

Gene Therapy (2007) **14,** 1249–1260; doi:10.1038/sj.gt.3302984; published online 21 June 2007

Keywords: *AAV; gene transfer; skeletal muscle; dog; immune response; Duchenne muscular dystrophy*

Introduction

Duchenne muscular dystrophy (DMD) is an X-linked, lethal disorder of skeletal muscle caused by mutations in the dystrophin gene, which encodes a large subsarcolemmal cytoskeletal protein, dystrophin. DMD is characterized by a high incidence (one among 3500 boys) and a high frequency of *de novo* mutation.[1] The absence of dystrophin accompanies the loss of dystrophin-associated glycoprotein complex from the sarcolemma and results in progressive muscle weakness, cardiomyopathy and early death. Although several treatment modalities, such as gene, cell and pharmacological therapies, have been researched to aim at correcting the dystrophic phenotypes, DMD currently has no effective treatment.

An adeno-associated virus (AAV) vector is a potential tool for gene therapy of inherited neuromuscular disorders. It is a nonpathogenic, low immunogenic and replication-defective viral vector that effectively infect nondividing cells, such as skeletal muscle fibers.[2] The size of exogenous DNA fragment which can be inserted into recombinant AAV vectors (rAAVs), however, is limited to up to 4.9 kb. Therefore, full-length dystrophin (14 kb) and mini-dystrophin (6.4 kb) cDNAs are too large to be incorporated into a rAAV. We and others have tried to design a short but functional microdystrophin gene that could be utilized as the therapeutic tool for DMD.[3–6] We constructed a series of rod-truncated microdystrophin cDNAs,[3] and generated transgenic *mdx* mice expressing each microdystrophin, and demonstrated that microdystrophin CS1 with four rod repeats and three hinges was a good candidate for therapeutic molecule.[7] We have also showed that the muscle-specific muscle creatine kinase (MCK) promoter in a rAAV drives longer transgene expression than the ubiquitous cytomegalovirus (CMV) promoter in *mdx* muscle.[8] Therefore, we generated the rAAV2 expressing microdystrophin ΔCS1 (3.8 kb cDNA) driven by the MCK promoter and introduced it into *mdx* muscles, and showed that sustained expression of microdystrophin from rAAV significantly ameliorates dystrophic phenotypes of

Correspondence: Dr S Takeda, Department of Molecular Therapy, National Institute of Neuroscience, National Center of Neurology and Psychiatry, 4-1-1 Ogawa-higashi, Kodaira, Tokyo 187-8502, Japan.
E-mail: takeda@ncnp.go.jp
Received 8 October 2006; revised 3 April 2007; accepted 14 May 2007; published online 21 June 2007